Science of the Total Environment xxx (2017) xxx–xxx

Contents lists available at ScienceDirect

Science of the Total Environment

journal homepage: www.elsevier.com/locate/scitotenv

Combination of experimental and *in silico* methods for the assessment of the phototransformation products of the antipsychotic drug/metabolite Mesoridazine

Marcelo L. Wilde [a], Jakob Menz [b], Christoph Leder [b], Klaus Kümmerer [b,*]

[a] Formerly: Sustainable Chemistry and Material Resources, Institute of Sustainable Environmental Chemistry, Leuphana University Lüneburg, C13, DE-21335 Lüneburg, Germany
[b] Sustainable Chemistry and Material Resources, Institute of Sustainable Environmental Chemistry, Leuphana University Lüneburg, C13, DE-21335 Lüneburg, Germany

HIGHLIGHTS

- Photolysis of the antipsychotic drug/metabolite MESO was simulated through Xe lamp.
- Sixteen TPs were detected and elucidated by means of an UHPLC-HRMS^n method.
- MESO and TPs were not readily biodegradable according to OECD 301D and 301F tests.
- Toxicity in bacteria decreased during photolysis proportionally to the concentration of MESO.
- *In silico* QSAR predicted the carbazole derivative TPs as PBT/vPvB and indicated positive alerts for mutagenicity.

GRAPHICAL ABSTRACT

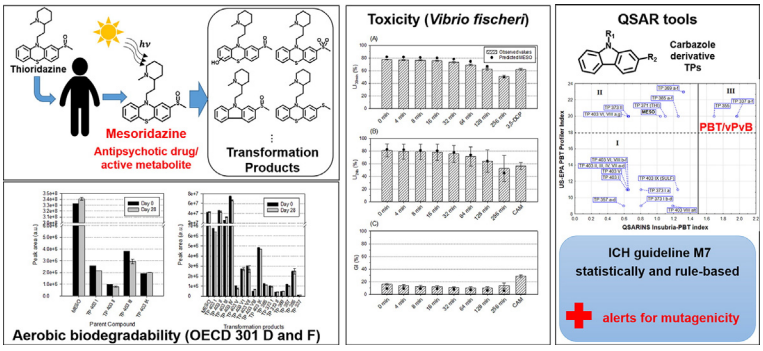

ARTICLE INFO

Article history:
Received 13 June 2017
Received in revised form 3 August 2017
Accepted 4 August 2017
Available online xxxx

Editor: D. Barcelo

Keywords:
Metabolite
Transformation products
Ready biodegradability
Ecotoxicity
QSAR
PBT/vPvB

ABSTRACT

The lack of studies on the fate and effects of drug metabolites in the environment is of concern. As their parent compounds, metabolites enter the aquatic environment and are subject to biotic and abiotic process. In this regard, photolysis plays an important role. This study combined experimental and *in silico* quantitative structure-activity relationship (QSAR) methods to assess the fate and effects of Mesoridazine (MESO), a pharmacologically active human drug and metabolite of the antipsychotic agent Thioridazine, and its transformation products (TPs) formed through a Xenon lamp irradiation. After 256 min, the photodegradation of MESO·besylate (50 mg L^{-1}) achieved 90.4% and 6.9% of primary elimination and mineralization, respectively. The photon flux emitted by the lamp (200–600 nm) was 169.55 J cm^{-2}. Sixteen TPs were detected by means of liquid chromatography-high resolution mass spectrometry (LC-HRMS), and the structures were proposed based on MS^n fragmentation patterns. The main transformation reactions were sulfoxidation, hydroxylation, dehydrogenation, and sulfoxide elimination. A back-transformation of MESO to Thioridazine was evidenced. Aerobic biodegradation tests (OECD 301 D and 301F) were applied to MESO and the mixture of TPs present after 256 min of photolysis. Most of TPs were not biodegraded, demonstrating their tendency to persist in aquatic environments. The ecotoxicity towards *Vibrio fischeri* showed a decrease in toxicity during the photolysis process. The *in silico* QSAR tools QSARINS and US-EPA PBT profiler were applied for the screening of TPs with character of persistence, bioaccumulation, and toxicity (PBT). They have revealed the carbazole derivatives TP 355 and TP 337 as PBT/vPvB (very persistent and very bioaccumulative) compounds. *In silico* QSAR predictions for mutagenicity and

* Corresponding author at: Nachhaltige Chemie und Stoffliche Ressourcen, Institut für Nachhaltige Chemie und Umweltchemie, Fakultät für Nachhaltigkeit, Leuphana Universität Lüneburg, Scharnhorststraße 1/C13, D-21335 Lüneburg, Germany.
E-mail addresses: marcelolw@gmail.com (M.L. Wilde), jakob.menz@uni.leuphana.de (J. Menz), cleder@leuphana.de (C. Leder), klaus.kuemmerer@uni.leuphana.de (K. Kümmerer).

https://doi.org/10.1016/j.scitotenv.2017.08.040

genotoxicity provided by CASE Ultra and Leadscope® indicated positive alerts for mutagenicity on TP 355 and TP 337. Further studies regarding the carbazole derivative TPs should be considered to confirm their hazardous character.

1. Introduction

The lack of studies on the fate and effects of drug metabolites in the environment is of great concern. The metabolism of drugs in humans involves typically the transformation of the parent drug into more polar and consequently more soluble compounds, which facilitate the drug elimination (Celiz et al., 2009; Santos et al., 2010). The presence of human metabolites has been demonstrated in environmental compartments and some of them in same concentration levels as the parent compounds (Langford and Thomas, 2011; López-Serna et al., 2013; Osorio et al., 2014).

Furthermore, once pharmaceuticals and their metabolites achieve wastewater treatment plants and surface waters, they are subject to natural attenuation processes, *i.e.* biotic and abiotic transformations (Zhu et al., 2015; Zonja et al., 2016). Biotic transformations are normally carried out by organisms such as bacteria and fungi leading to its complete mineralization or the formation of unknown transformation products (TPs) (Fatta-Kassinos et al., 2011; Kümmerer, 2010, 2009). Photolysis is an important abiotic process and plays a major role in the environmental fate of pharmaceuticals and their metabolites. In general, pharmaceuticals and metabolites possess structural moieties, which are able to absorb sunlight radiation leading to direct and indirect (sensitized) photolysis (Du et al., 2014; Fatta-Kassinos et al., 2011; Lin et al., 2013).

An increase in toxicity due to the formation of a more toxic cocktail of TPs by photolysis has been reported in several studies (Wang and Lin, 2014; Mahmoud et al., 2014; Herrmann et al., 2015). This chronic exposure to residues of pharmaceutical, metabolites, and TPs can generate subtle effects on aquatic organisms and in a risk to human health by consumption of contaminated waters and even through contaminated food (Paltiel et al., 2016; Vandermeersch et al., 2015; Wu et al., 2014).

Many human metabolites and TPs still contain structural similarities to the parent compounds and present pharmacophore groups attaining similar activity (Cwiertny et al., 2014; Fura, 2006). Besides, photodegradation might not entirely change the pharmacophore structure of the parent compound. Zhu et al. (2015) pointed out that the photodegradation of amlodipine (AML), diltiazem (DIL), and verapamil (VER) under UV (254 nm) irradiation led to TPs still containing intact pharmacophore structures. The TPs of VER did not present ecological risks. Conversely, the photodegradation of AML and DIL under typical of disinfection UV fluence led to TPs containing pharmacophores, which could present potential risks. Therefore, photodegradation of pharmaceuticals might not entirely eliminate the risk of pharmaceuticals in the environment.

Many drug metabolites have been studied and identified within pharmaceutical drug development and the ones that retained a pharmacological activity have often attained importance as pharmaceuticals. Mesoridazine (MESO, or Thioridazine-2-sulfoxide) is such an example. It is a phenothiazine-derived antipsychotic agent and a major metabolite of Thioridazine in humans and animals. MESO is formed through a sulfoxidation on the R2-substituent (SCH_3) at the C2-position of the phenothiazine tricyclic ring. In the human body, approximately 30% of orally administered THI is excreted in the urine and 50% of the original dose is excreted in the feces (Eiduson and Geller, 1963). The mean total excretion of MESO in the urine of humans is 6.3% (Hawesx, 1993).

Owing to a higher antipsychotic activity than Thioridazine (Obach, 2013; Ravyn et al., 2013), MESO was proposed for treatment of psychotic disease such as schizophrenia. Nevertheless, some unwanted side effects have been found such as cardiac toxicity and QT-prolongation, which has led to a withdrawal in some countries (Jin et al., 2014). On the other hand, Thioridazine is still used in antipsychotic therapy and has been found as a potent antimicrobial agent (Amaral, 2012; Thanacoody, 2007, 2011). This could lead to an elevated environmental occurrence of MESO and possible resulting TPs. The photostability of MESO under UV light of 254 nm and 366 nm was tested in methanolic solutions and epimerization of was observed (De Gaitani et al., 2004), but no extensive study on the environmental fate and effects of the photolysis of MESO has been reported yet in the literature. Besides, MESO was also identified as a TP of the parent compound Thioridazine in our previous studies of photolysis and Fenton process (Wilde et al., 2017, 2016).

The assessment of the photolytic fate of human metabolites and their TPs is even more scarce in the literature (Bonvin et al., 2013). Therefore, the aim of the present study was to assess the fate and effects of the TPs formed from the antipsychotic and human metabolite MESO through a Xenon lamp irradiation. The elucidation and proposal of the chemical structure of TPs were carried out by means of ultra-high performance liquid chromatography tandem high-resolution Orbitrap mass spectrometry (UHPLC-HRMS). The fate and effects of MESO and irradiated solutions were tested experimentally by means of ready biodegradability according to OECD 301D and 301F tests, and the toxicity was tested towards luminescent bacteria (*Vibrio fischeri*). *In silico* models based on quantitative structure-activity relationships (QSAR) were applied to screen for TPs with the character of persistence, bioaccumulation, and toxicity (PBT). Furthermore, QSAR models were also employed for the prediction of genotoxic and mutagenic activities of identified TPs.

2. Materials and methods

2.1. Chemicals

Mesoridazine besylate (MESO·besylate, CAS Nr. 32672-69-8) was acquired from Santa Cruz Biotechnology (Dallas, Texas, USA). 3,5-Dichlorophenol (97%, CAS Nr. 591-35-5), Chloramphenicol (98%, CAS Nr. 56-75-7) were purchased from Sigma-Aldrich (Deisenhofen, Germany). Benzenesulfonic acid sodium salt (*i.e.* besylate) (98%, CAS Nr. 515-42-4) was acquired from Acros Organics (New Jersey, USA). Organic solvents were of LC-MS grade and provided by VWR (Darmstadt, Germany). Aqueous solutions were prepared in ultrapure water (Q1:16.6 MΩ·cm and Q2:18.2 MΩ·cm, Ultra Clear UV TM, Barsbüttel, Germany). All other chemicals used were of recognized analytical grade.

2.2. Photolysis setup

The photolysis experiments were carried out in a 1000 mL cylindrical immersion-type batch reactor. The irradiation was simulated by means of a UV/VIS 150 W Xenon lamp (TXE 150 W, UV Consulting Peschl, Mainz, Germany) surrounded by an ilmasil quartz glass used as a cooling jacket separating the lamp from the solution immersed into a 800 mL of synthetic solution of MESO diluted in ultrapure water (Text S1, Supplementary material). The irradiation of the lamp, measured with a Black Comet UV-VIS spectroradiometer model C (StellarNet Inc., Florida, USA), was: 200–280 nm: 1.01 W m^{-2}; 280–315 nm: 3.29 W m^{-2}; 315–380 nm: 12.91 W m^{-2}, 380–850 nm: 243.16 W m^{-2}. The spectrum of the lamp and the molar extinction

Please cite this article as: Wilde, M.L., et al., Combination of experimental and *in silico* methods for the assessment of the phototransformation products of the antipsychotic drug/metabolite Mesoridazine, Sci Total Environ (2017), https://doi.org/10.1016/j.scitotenv.2017.08.040

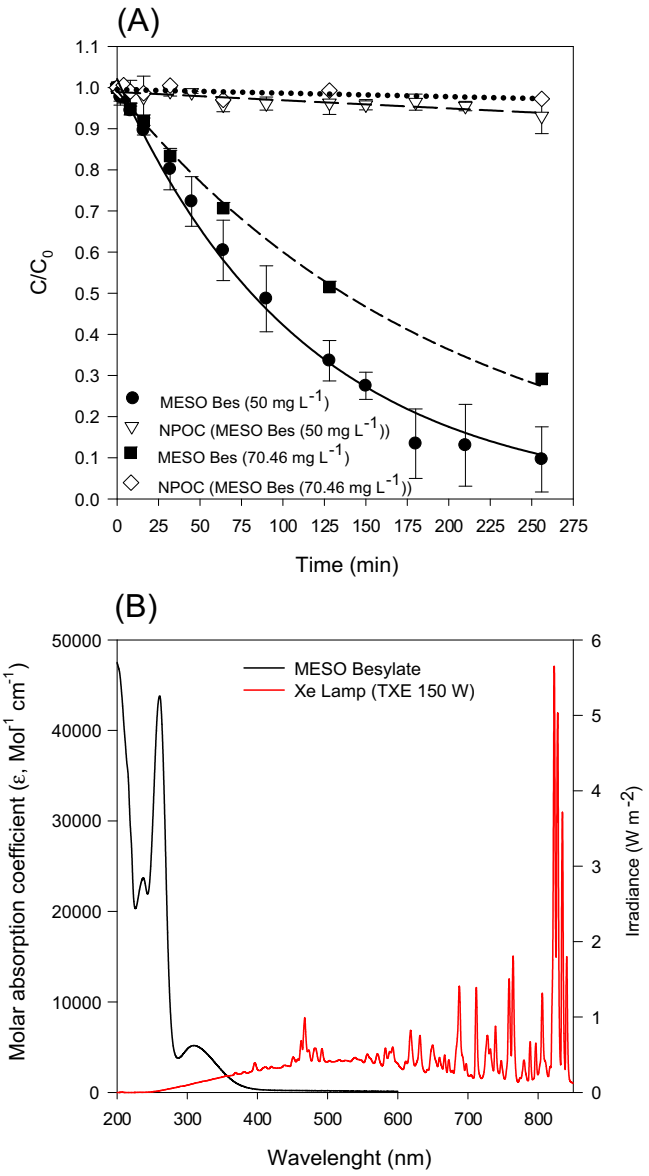

Fig. 1. (A) Non-purgeable organic carbon (NPOC) removal and primary elimination of Mesoridazine (MESO) through photolysis by means of Xe lamp (TXE 150 W) irradiation. Initial conditions: [MESO·besylate] 50 mg L^{-1} (35.48 mg L^{-1} of MESO only), pH 7.0, temp.: 20 ± 2 °C ($n = 2$); [MESO·besylate] 70.46 mg L^{-1} (50.00 mg L^{-1} of MESO only), pH 7.0, temp.: 20 ± 2 °C ($n = 1$). (B) Irradiance (W m^{-2}) of the Xenon lamp (TXE 150 W) and molar absorption coefficient of MESO·besylate (ε_{PPL}).

coefficient of MESO are depicted in Fig. 1 (B). The initial concentration of MESO·besylate used in the experiments were 50 mg L^{-1} (corresponding to 35.48 mg L^{-1} of MESO) and 70.46 mg L^{-1} (50.00 mg L^{-1} of MESO). They were chosen in order to allow the detection of as many TPs as possible and further experimental evaluation of aerobic biodegradation and toxicity tests, respectively. The experiments were carried out at pH 7 and no adjustments in pH of the solution were carried out during and after the experiments. The temperature was held at 20 ± 2 °C with a circulating cooler (WKL230, LAUDA, Berlin, Germany).

2.2.1. Kinetics of degradation and quantum yield calculations

In general, a photochemical reaction does not follow a specific reaction order, but the kinetic behavior dependent on the absorption conditions of the target compound (Oppenländer, 2003). Thus, a first-order kinetic model was proposed to fit the exponential decay of MESO according to Eq. (1):

$$C = C_0 \cdot e^{-k_{obs} t} \quad (1)$$

where C is the concentration of MESO during the photolysis, C_0 is the initial concentration of MESO, k_{obs} is the observed kinetic constant, t is irradiation time. The half-life ($t_{½}$) was calculated according to Eq. (2):

$$t_{1/2} = {}^{0.693}/_{k_{obs}} \quad (2)$$

The kinetics of the experimental data were fitted with the software SigmaPlot 12 (Systat Software, USA) by means of nonlinear model fit regressions. The statistical analysis of the fitting was performed by means of ANOVA.

The quantum yield for MESO was calculated using the modified equation for polychromatic irradiation sources (Eq. (3)) (Zepp, 1978; Zepp and Cline, 1977).

$$\Phi_{MESO} = \frac{k_{obs}}{2.303 \times \sum_{600}^{200} I_{0\lambda} \epsilon_\lambda \times l \times \left(\frac{A}{V}\right)} \quad (3)$$

where $\varnothing_{MESO}$ is the apparent quantum yield (mol $Einstein^{-1}$) of MESO, k_{obs} is the kinetic constant of primary elimination (s^{-1}). The term $\sum_{\lambda_i}^{\lambda_n} I_{0\lambda}\epsilon_\lambda$ is the sum of the spectral superposition of the irradiation emitted by the lamp on the target compound at a determined wavelength range. Thus, $I_{0\lambda}$ is the spectral photon flux rate at each wavelength from 200 to 850 nm (Einstein m^{-2} s^{-1}), ϵ_λ is the molar extinction coefficient of MESO (m^{-2} mol^{-1}), l is the radiation pathway from the lamp to solution bulk (0.015 m), A is area of reactor (0.062 m^2), and V is the volume of reactor (0.0011 m^3).

The spectral photon flux rate of the lamp was calculated according to Eq. (4).

$$I_\lambda = \frac{E \cdot \lambda \cdot 5.03 \cdot 10^{15}}{N_A} \quad (4)$$

where E is the irradiance of the lamp (W m^{-2}), λ is the wavelength (m), N_A is Avogadro's number (6.022 × 10^{23} mol^{-1}), and 5.03 × 10^{15} m^{-2} s^{-1} is a constant.

2.3. Instrumental analysis

The primary elimination was measured by HPLC-DAD-FLD Prominence HPLC (Shimadzu, Duisburg, Germany) according to the modified method of Trautwein and Kümmerer (2012a). A non-target approach was performed for the detection and elucidation of TPs using an Agilent Technologies HPLC 1100 series (Agilent Technologies, Böblingen, Germany) tandem Mass Spectrometer Esquire 6000^{plus} Ion Trap with atmospheric pressure electrospray ionization (ESI) interface (Bruker Daltonics GmbH, Bremen, Germany) in positive ion mode (LC-ESI-IT-MS^n). A more accurate elucidation of the TPs was proposed by using a Dionex Ultimate 3000 UHPLC system (Dionex, Idstein, Germany) tandem to an LTQ Orbitrap-XL high-resolution mass spectrometer (HRMS) with H-ESI ion source (Thermo Scientific, Bremen, Germany). The chromatographic separation in both LC-MS/MS instruments was carried out on a reverse phase column C18 ec RP18 CC 125-2 mm Nucleodur 100-3 and guard column RP18 CC 8–2 mm Nucleodur 100-3 (Macherey-Nagel, Düren, Germany). Detailed information the chromatographic methods can be found in Text S2 (Supplementary material).

The mineralization was determined by monitoring the non-purgeable organic carbon (NPOC) through a total organic carbon analyzer (TOC-Vcpn, Shimadzu GmbH, Duisburg, Germany) with ASI-V auto-sampler.

Please cite this article as: Wilde, M.L., et al., Combination of experimental and *in silico* methods for the assessment of the phototransformation products of the antipsychotic drug/metabolite Mesoridazine, Sci Total Environ (2017), https://doi.org/10.1016/j.scitotenv.2017.08.040

2.4. Aerobic biodegradation tests

MESO·besylate and the mixture resulting after 256 min of photodegradation were submitted to Closed Bottle Test (CBT) (OECD 301 D) and Manometric Respirometry Test (MRT) (OECD 301F) according to the OECD guidelines (OECD, 1992). The CBT was carried out by using low nutrient load and low bacteria density (10^2–10^5 CFU mL^{-1}) (OECD, 1992), in the dark at 20 (±1) °C for a period of 28 days. The oxygen demand (OD) was measured by a sensor Fibox 3 (Presens, Regensburg, Germany) (Friedrich et al., 2013). The MRT was performed by using an OxiTop® OC-110 system (WTW, Weilheim, Germany) under constant stirring in the dark during 28 days at 20 (±1) °C and using the same mineral medium as for CBT (OECD, 1992). The inoculum used was a sample of effluent from the municipal STP Lüneburg (Abwasser, Grün & Lüneburger Service GmbH (AGL), Lüneburg, Germany), which serves a regional population equivalent of 144,000 inhabitants. Further information can be found in Text S3 (Supplementary material). The peak area analysis of MESO and TPs was carried out at day 0 and after 28 days by LC-ESI-IT-MS^n (see Section 2.3).

2.5. Assessment of the toxicity by modified luminescent bacteria test

The toxicity on bacteria was assessed in a modified luminescent bacteria test (LBT) with *Vibrio fischeri* NRRL-B-11177 (Hach-Lange GmbH, Düsseldorf, Germany) according to (Menz et al., 2013). This bioassay was specially designed for the combined determination of short-term (30 min) and long-term (24 h) inhibition of bacterial bioluminescence. In addition, the inhibition of bacterial growth was evaluated at the transition to the stationary phase after 14 h incubation. Detailed information about the experimental procedure of the LBT can be found in Text S4 (Supplementary material). Inhibitory effects were determined in relation to a nonexposed control. A minimum threshold of 20% inhibition was applied for the identification of significant effects. The fitting of concentration-response curves was done with the software package SigmaPlot 11 (Systat Software) using a four-parameter Hill model (Eq. (5)).

$$y = min + (max - min)/\left(1 + (x/EC_{50})^{-Hillslope}\right) \quad (5)$$

where min is the bottom of the curve, max is the top of the curve, *Hillslope* is the slope of the curve at its midpoint and EC_{50} is the half-maximal effective concentration. The expected effect of MESO in the photolysis mixture was predicted by inserting the measured concentration of MESO into the plot equation of the fitted concentration-response curve.

2.6. In silico quantitative structure-activity relationships (QSARs) predictions

The neutral species (*i.e.* not considering protonated, deprotonated and/or zwitterion microspecies) of the chemical structures investigated were converted into the simplified molecular-input line-entry system (SMILES) and subjected to *in silico* predictions. The QSARINS software v.2.0 (Gramatica et al., 2014, 2013) based on the Insubria-PBT Index (Papa and Gramatica, 2010) as implemented in the QSARINS-Chem module of the software QSARINS and the US-EPA PBT Profiler v.2.000 (USEPA, 2012) were used in a consensus mode for the screening of PBT compounds. Moreover, two other QSAR platforms were used for the prediction of mutagenic and genotoxic activities: CASE Ultra (v. 1.6.0.3 MultiCASE Inc.) (Chakravarti et al., 2012; Saiakhov et al., 2013; Saiakhov et al., 2014) and Leadscope® (v. 3.4.2-2) (Roberts et al., 2000). The applied models included both statistical and rule-based systems as recommended by the ICH M7 guidelines (International Conference on Harmonization (ICH), 2014) to predict mutagenicity and were used for different endpoints as can be seen in Text S5 (Supplementary material).

3. Results and discussion

3.1. Photolysis

The photon flux emitted by the lamp (wavelength range 200–600 nm) during 256 min of irradiation was 169.55 J cm^{-2}. Fig. 1 (A) shows that the photolysis achieved 90.4% (±7.9%) of primary elimination and 6.9% (±4.2%) of mineralization after 256 min for the initial concentration of 50 mg L^{-1} MESO·besylate (35.48 mg L^{-1} of MESO). For the initial concentration of 70.46 mg L^{-1} MESO·besylate (50.00 mg L^{-1} of MESO), the photolysis reached after 256 min of photolysis was 70.8% of primary elimination and only 2.75% of mineralization. These results indicated that the photolysis was a mere transformation process, reinforcing the need to measure mineralization in photolysis experiments and to include results from the assessment of fate and effects of TPs in the environment.

As depicted in Fig. 1 (A), the NPOC removal was fitted with the zero-order kinetic model with $k_{DOC_{obs}}$ 3.43×10^{-6} mol L^{-1} s^{-1} (95% confidence interval (CI): $[2.29 \times 10^{-6} - 4.57 \times 10^{-6}]$) and r^2 0.784 ($p < 0.05$) for the initial concentration of 50.00 mg L^{-1} MESO·besylate (29.76 mg L^{-1} of organic C). The zero-order kinetic constant for the initial concentration of 70.46 mg L^{-1} MESO·besylate (41.94 mg L^{-1} of organic C) was $k_{DOC_{obs}}$ 1.47×10^{-6} mol L^{-1} s^{-1} (95% CI: $[-3.76 \times 10^{-7} - 3.31 \times 10^{-6}]$) and r^2 0.339 ($p = 0.1018$). The primary elimination of MESO was fitted by a first-order exponential decay for both concentration studied as showed in Fig. 1 (A). The computed kinetic constant for the photolysis of MESO (35.48 mg L^{-1}) was k_{obs} 1.47×10^{-4} s^{-1} (95% CI: $[1.35 \times 10^{-4} - 1.59 \times 10^{-4}]$) with r^2 0.993 ($p < 0.05$), with a half-life time ($t_{½}$) of 4861.2 s. Considering MESO (50.00 mg L^{-1}) the k_{obs} 8.39×10^{-5} s^{-1} (95% CI: $[7.95 \times 10^{-5} - 8.83 \times 10^{-5}]$) with r^2 0.998 ($p < 0.05$) and the half-life time ($t_{½}$) was 8179.2 s.

The apparent quantum yield of MESO (Φ_{MESO}) at pH 7 was estimated to be 3.05×10^{-6} ($\pm 6.37 \times 10^{-7}$) mol Einstein^{-1} ($n = 2$) using the kinetic slope method (Zepp, 1978; Zepp and Cline, 1977). At the pH 7, the major species of MESO was calculated to be 93.95% of the tertiary amine of the piperidine moiety protonated; whereas 6.05% are estimated to be neutral (calculated using Marvin 6.0.3, 2013, (ChemAxon, http://www.chemaxon.com). The monitoring of the pH during the photolysis showed no perceptible changes in pH (see Text S6, Supplementary material). The phototransformation of MESO occurs by either direct or indirect photolysis. In the direct photolysis, the absorbance of photons plays an important role. The photolysis depends on both, the rate of light absorption and the reaction quantum yield of the excited state. As observed in Fig. 1 (B), the emission of the lamp overlaps the absorbance of MESO in the range of 280–400 nm.

A hypothesized scheme concerning the possible pathways of MESO through photolysis was proposed (Fig. 2). MESO can follow different pathways under irradiation: (i) MESO in a competition with intersystem crossing can undergo photoionization through direct photolysis

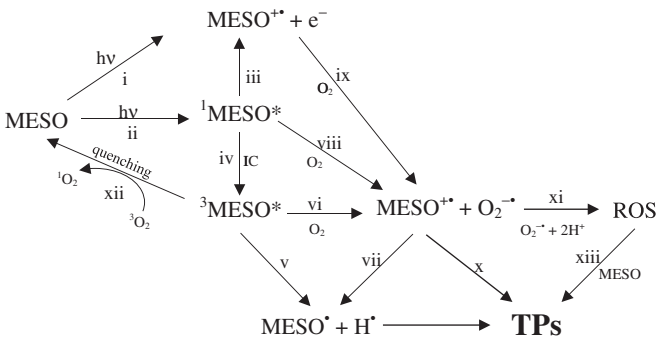

Fig. 2. Hypothesized reaction scheme for the direct photolysis of Mesoridazine (MESO) in aqueous solution in presence of natural dissolved oxygen. ROS: reactive oxygen species; TPs: transformation products.

forming MESO cation radical ($MESO^{+}$•) and a hydrated electron (Rodrigues et al., 2006), which in the presence of dissolved oxygen can further form superoxide (O_2^-•) (ix). However, direct photoionization is unlikely to occur according to energetic considerations (Fasnacht and Blough, 2002). Likewise, MESO is excited to a singlet state (^{1}MESO*) (ii), where it can undergo intersystem crossing (IC) *via* internal conversion to a triplet state (^{3}MESO*) (iv) by a biphotonic or monophotonic absorption process (Rodrigues et al., 2006), or, in the presence of dissolved oxygen, it might form an $MESO^{+}$• and O_2^-• (viii). The $MESO^{+}$• can further form TPs (x) and reactive oxygen species (ROS) (xi), or as proposed by Rodrigues et al. (2006) lead to the formation of MESO• and H• (vii). Alternatively, the singlet state ^{1}MESO* might also undergo photoionization forming $MESO^{+}$• and hydrated electron (iii). Likewise, the triplet state ^{3}MESO* can lead to the formation of MESO• and H• through monophotonic homolytic cleavage (v), $MESO^{+}$• and O_2^-• (vi), or even be quenched by triplet oxygen (xii) returning to the ground state of MESO (Fasnacht and Blough, 2002).

The singlet oxygen in photolysis has been pointed out as a very important variable in the direct photolysis studies (Chen et al., 2008; Du et al., 2014; Edhlund et al., 2006). Chen et al. (2008) have proposed that oxygen singlet is formed through the quenching of triplet state of MESO.

The indirect photolysis of MESO should be considered as well, and it could be based on the self-sensitization process. Self-sensitization of phenothiazine derivatives has been pointed out in the study of monochromatic photolysis of *N*-methyl phenothiazine (Manju et al., 2012). In general, self-sensitization is concentration dependent, commonly occurring in higher concentrations of the target compound (Werner et al., 2006). Therefore, the formation of ROS ($^1O_2$, HO_2•, and H_2O_2) should not be neglected as proposed by the pathway (xiii) in Fig. 2. Chen et al. (2008) have investigated the formation of $^1O_2$ in the photolysis of tetracycline under simulated sunlight conditions, detected $^1O_2$ over a wide pH range, with an increase with the of irradiation time. Besides, the formation of H_2O_2 in simulated sunlight conditions was also identified and proposed to be generated through the O_2^-• formation (Chen et al., 2008). On the other hand, Kelly and Arnold (2012) have investigated the self-sensitization of phytoestrogens and the generation of $^1O_2$ during photolysis. They could not detect $^1O_2$ and argued that such behavior might be due to lower energy and short-lived triplet states of the parent compounds. In their study dissolved oxygen acted mainly as a triplet quencher making direct photolysis the main photolytic pathway (Kelly and Arnold, 2012). It has also been proposed that self-sensitization processes are unlikely to happen at environmental concentrations of the parent compounds (Wammer et al., 2013). On the other hand, in the aquatic environment, indirect photolysis occurs due to the presence of other molecules such as dissolved organic matter including humic acids and fulvic acids as well as nitrate or carbonate that can act as sensitizers under sunlight leading to ROS (Jacobs et al., 2012; Li et al., 2016; Lin et al., 2013).

3.2. Identification of TPs and proposal of degradation pathway

A non-target approach and data-dependent acquisition (combination of full scan and product ion spectra) were applied for the identification of transformation products. The samples collected at predetermined times were analyzed by a full scan from 60 to 500 *m/z* in positive ion mode. A resolving power of 30,000 FWHM was used. The most intense ion of the full scan was isolated and further fragmented (MS^2) and the two most intense product ions of MS^2 were isolated and further fragmented (MS^3). A suspect screening list with specific masses of the most probable TPs was used in the data-dependent acquisition, whereas in the non-target approach the most intense ion was activated if no parent masses were found. The total ion chromatograms, fragmentation patterns (up to MS^3) and proposed structures of the TPs can be seen in Text S7 and Text S8 (Supplementary material).

Sixteen TPs were found resulting from photolysis. Chromatographic peaks with the same *m/z* $[M + H]^+$ and different retention times were observed, indicating the formation of constitutional isomers. A possible photolysis pathway based on these results is shown in Fig. 3. Nine peaks with the *m/z* $[M + H]^+$ 403 Da were found indicating sulfoxidation or mono-hydroxylation. Based on the product ion of *m/z* 292.0461 ($C_{14}H_{14}O_2NS_2$) and 142.1224 ($C_8H_{16}ON$) indicating that the hydroxylation on TP 403 I might occur on the α-carbon of the R1-substituent of MESO. TPs 403 II-V and VII have also presented the product ion of *m/z* 142.1224 ($C_8H_{16}ON$) in the MS^2 and/or MS^3 spectra, but accordingly to the fragmentation pattern the hydroxylation was proposed on the piperidine moiety.

The exact position of the hydroxylation cannot be given based on the MS^n data only. The fragmentation pattern of TPs 403 VI and VIII indicated that the hydroxylation happened at an aromatic ring of the tricyclic phenothiazine ring. TP 403 IX was proposed to undergo a new sulfoxidation on the R2-substituent forming Thioridazine-2-Sulfone (Sulforidazine). The loss of the moiety $S(O_2)CH_3$ evidenced by the product ion of *m/z* 324.1656 ($C_{20}H_{24}N_2S$) supported this proposition. Sulforidazine has been proposed as a metabolite of both Thioridazine and Mesoridazine (Borges et al., 2007; De Gaitani et al., 2004; Eap et al., 1996; Hawesx, 1993; Wójcikowski et al., 2006) and is considered pharmacologically active as well (Borges et al., 2007).

Hydrogen abstraction or dehydroxylation have also taken place forming the TP 385. Due to the absence of the product ion of *m/z* 126, the formation of a double bond was proposed to occur on the piperidine moiety. Two peaks with the same *m/z* $[M + H]^+$ of 373 Da were found, and based on the HRMS two different structures were proposed. TP 373 I (exact *m/z* $[M + H]^+$ 373.1573 Da) was proposed to present the formula $C_{20}H_{25}O_3N_2S$ (Δmmu error of −0.780) and be formed by losing the side chain $S(O)CH_3$ and present the formation of sulfone in the S5-position followed by a hydroxylation on the phenothiazine ring. The product ion of *m/z* 260.0378 ($C_{13}H_{10}O_3NS$) support the proposed structure by presenting the three oxygens on the phenothiazine ring, whereas fragmentation pattern considering the MS^2 product ions of *m/z* 293.2015 ($C_{20}H_{25}N_2$), 180.0813 ($C_{13}H_{10}N$) and MS^3 product ion of *m/z* 179.0730 ($C_{13}H_9N$) indicated the loss of $S(O_2)$. On the other hand, TP 373 II (exact *m/z* $[M + H]^+$ 373.1402 Da) was proposed to present the formula $C_{20}H_{25}ON_2S_2$ (Δmmu error of −0.111) and is assumed to be formed through an *N*-demethylation on the piperidine moiety: the MS^2 and MS^3 product ion of *m/z* 112.1122 Da ($C_7H_{14}N$) indicated the loss of CH_3 in the R1-substituent.

The TP 371 was proposed to be Thioridazine as they have identical fragmentation patterns (Text S8, Supplementary material). Formation of Thioridazine evidences occurrence of an abiotic back-transformation process in the photolysis of metabolites and it might be assumed to take place in the environment as well. Back-transformation of metabolite to parent compound through photolysis have also been reported in the photolysis from the metabolite 4-nitroso-sulfamethoxazole back to sulfamethoxazole (Bonvin et al., 2013). A further dehydrogenation step of MESO takes place forming the TP 369. It is not possible to state the exact position of the double bond in TP 369 based on the MS^n data only. The formation of TP 369 was also reported in the photolysis of Thioridazine (Wilde et al., 2016). The TP 357 with the exact of *m/z* $[M + H]^+$ 357.1632 Da and calculated elemental composition $C_{20}H_{25}O_2N_2S$ (Δmmu error of 0.065) is proposed to be formed through sulfoxidation in the S5-position of the tricyclic phenothiazine ring followed by a hydroxylation of an aromatic ring. The fragmentation pattern obtained by HCD provided the product ion of *m/z* 126.1278 Da ($C_8H_{16}N$) indicating that the R1-substituent was intact and the R2-substituent ($S(O)CH_3$) was eliminated, whereas the product ion of *m/z* 232.0430 Da ($C_{12}H_{10}O_2NS$) provided the information that sulfoxidation and hydroxylation occurred on the tricyclic phenothiazine ring.

Two carbazole ring derivatives were found during the photolysis of MESO, TP 355 and TP 337 (exact *m/z* $[M + H]^+$ 355.1841 Da and $[M + H]^+$ 337.1727 Da, elemental composition, calculated formula

Please cite this article as: Wilde, M.L., et al., Combination of experimental and *in silico* methods for the assessment of the phototransformation products of the antipsychotic drug/metabolite Mesoridazine, Sci Total Environ (2017), https://doi.org/10.1016/j.scitotenv.2017.08.040

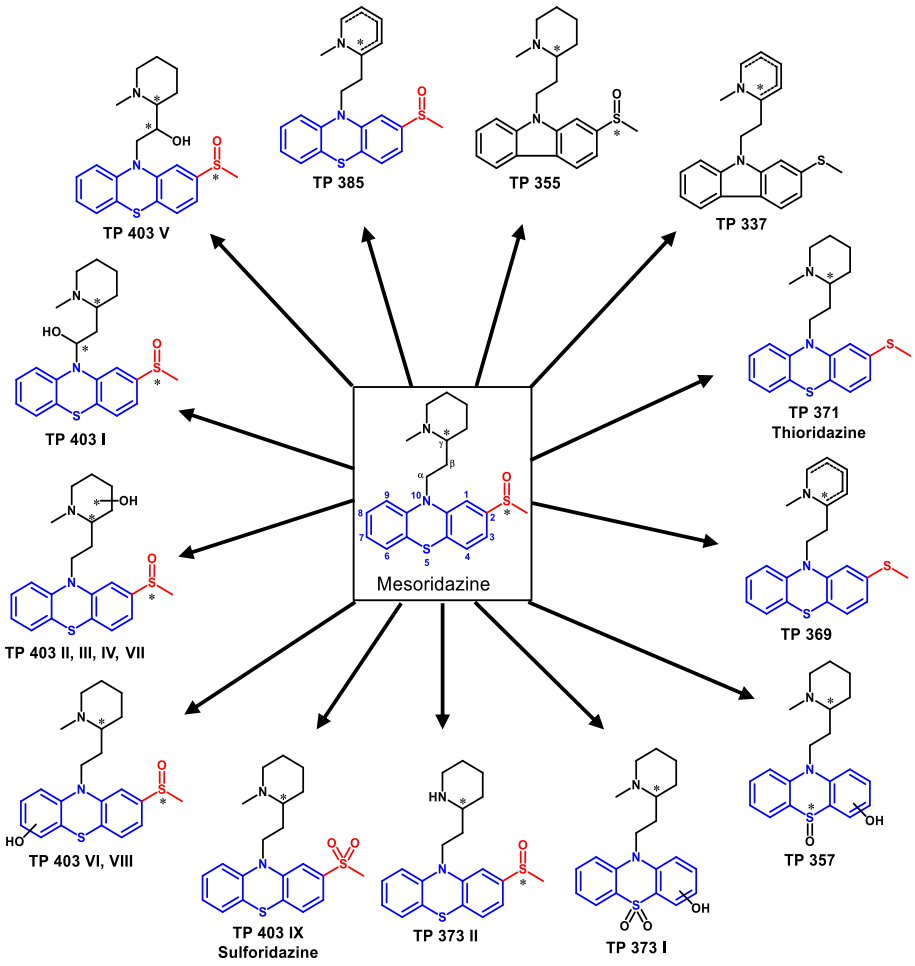

Fig. 3. Proposed photolysis pathway of MESO under Xe lamp irradiation. * means the chiral centers.

$C_{21}H_{27}ON_2S$ (Δmmu error of 0.249) and $C_{21}H_{25}N_2S$ (Δmmu error of −0.626), respectively). In accordance with their fragmentation patterns, a sulfoxide elimination on the S5-position can be assumed for both TPs. Carbazole derived TPs were also found in the photolysis of Thioridazine (Wilde et al., 2016) through sulfoxide elimination. The formation of a carbazole ring during photolysis was reported for the photolysis of *N*-methyl phenothiazine (Manju et al., 2012) and in the photolysis of diclofenac (Musa and Eriksson, 2009). Besides, carbazole-derived TPs were also identified in a previous work regarding the photolysis of Thioridazine in the same conditions (Wilde et al., 2016), indicating that both parent compound (Thioridazine) and its human metabolite (Mesoridazine) can lead to carbazole-derivative compounds by long-term exposition to irradiation.

With exception of TP 373 I, TP 357, TP 355, and TP 337 the photolysis of MESO have not produced many changes in the pharmacophore structure of the phenothiazine pharmaceuticals. Phenothiazine pharmaceuticals are composed of the phenothiazine tricyclic ring (represented in blue), an alkyl substituent on N10-position (represented in black), and an electron withdrawing group bonded to C2-position (represented in red) (Jaszczyszyn et al., 2012). However, the ring substitutions interfere in the antipsychotic activity, being that the substitution on C1- and C4-position interfere in the bending of the side chain and the S-binding affinity towards the receptor, respectively (Alagarsamy, 2010; Sriram and Yogeeswari, 2010). More than one substitution on the phenothiazine ring decreases the antipsychotic potency (Alagarsamy, 2010; Sriram and Yogeeswari, 2010), *i.e.* although speculative, TP 403 VI, VIII might be less potent than MESO and Thioridazine. The oxidation on the S5-position to sulfoxide and sulfone decreases the activity (Wójcikowski et al., 2006) and, consequently, TP 357 and TP 373 I can be expected as of less potency. Besides, the hydroxyl group is also a strong electron-donating group contributing to reduce the activity.

The alkyl side chain modulates the pharmacological antipsychotic activity (Faria et al., 2015). The substitution on the α-C tends to decrease the antipsychotic potency (Alagarsamy, 2010; Sriram and Yogeeswari, 2010). Thus, it is expected that TP 403 I presents lower potency that MESO. Depending on the substituent in the β-C, it might increase or decrease the activity (Alagarsamy, 2010; Sriram and Yogeeswari, 2010). Therefore, TP 403 V might also have activity. Phenothiazines with the tertiary amino group have high potency (Jaszczyszyn et al., 2012) and, consequently, TP 373 II might present lower potency than MESO. Likewise, TP 403 II-IV, VII that was proposed to undergo hydroxylation on the piperidine moiety and TP 385 and TP 369 with a proposed double bond in the piperidine moiety could also present higher or lower activity than MESO and Thioridazine, which would need further tests to evaluate it.

According to the TPs proposed, the photolysis of MESO leads to new chiral compounds, which can possess different pharmacological activities and toxicities (Kasprzyk-Hordern, 2010). Mesoridazine has two chiral centers and the photolysis lead to both the loss of one chiral center and to the formation of TPs with new chiral centers. The formation of TPs 403 I—V and VII present a new chiral center in the piperidine moiety. This third chiral point occurs in the position that the hydroxylation takes place at α- or β-carbon. The formation of TPs 403 VI and VIII, TP 385, TP 373 II, TP 357 and TP 355 maintained the same number of chiral center as the parent compound. On the other hand, the formation of TP 403 X, TP 373 I, TP 371 (Thioridazine), TP 369, and TP 337 present a loss

Please cite this article as: Wilde, M.L., et al., Combination of experimental and *in silico* methods for the assessment of the phototransformation products of the antipsychotic drug/metabolite Mesoridazine, Sci Total Environ (2017), https://doi.org/10.1016/j.scitotenv.2017.08.040

of one chiral center. Besides, TP 385, TP 369, and TP 357 depending on the position of the double bond in the piperidine moiety might lose the chiral center.

Thioridazine is used as a racemate, but the (*R*)-enantiomer has been shown to be 2.7 times more potent than the (*S*)-enantiomer of binding to the D2 dopamine receptor, and nearly five times more potent than alpha-1 receptor antagonist (Choi et al., 2004; Leonard, 2003). On the other hand, the S-isomer has a 10-fold greater affinity for the D1 receptor than the R-form. Besides, dose-response relationship showed that the racemate is 12 times more potent than S-isomer and 3 times more potent than the R-isomer (Leonard, 2003). The enantiomers of MESO have shown different binding affinities towards different receptors as well, and the stereochemistry of the sulfoxide moiety was shown to play an important role in the structure-activity relationship (Choi et al., 2004).

Fig. 4 shows the normalized chromatographic peak area ratio A/A_0 (%), where A is the relative peak area of the TP and A_0 is the relative peak area of MESO before photolysis. Although it is not possible to relate the peak area ratio with a concentration in the case of TPs since no standards are available, it is possible to relate the peak area ratio with the formation and further transformation of TPs during the photolysis. Thus, TP 403 III, IV and V have achieved up to 15.6%, 8.4%, and 19.8% of the initial area of the parent compound, respectively. As observed, most of the TPs presented a tendency in increase the peak area with the evolution of photolysis.

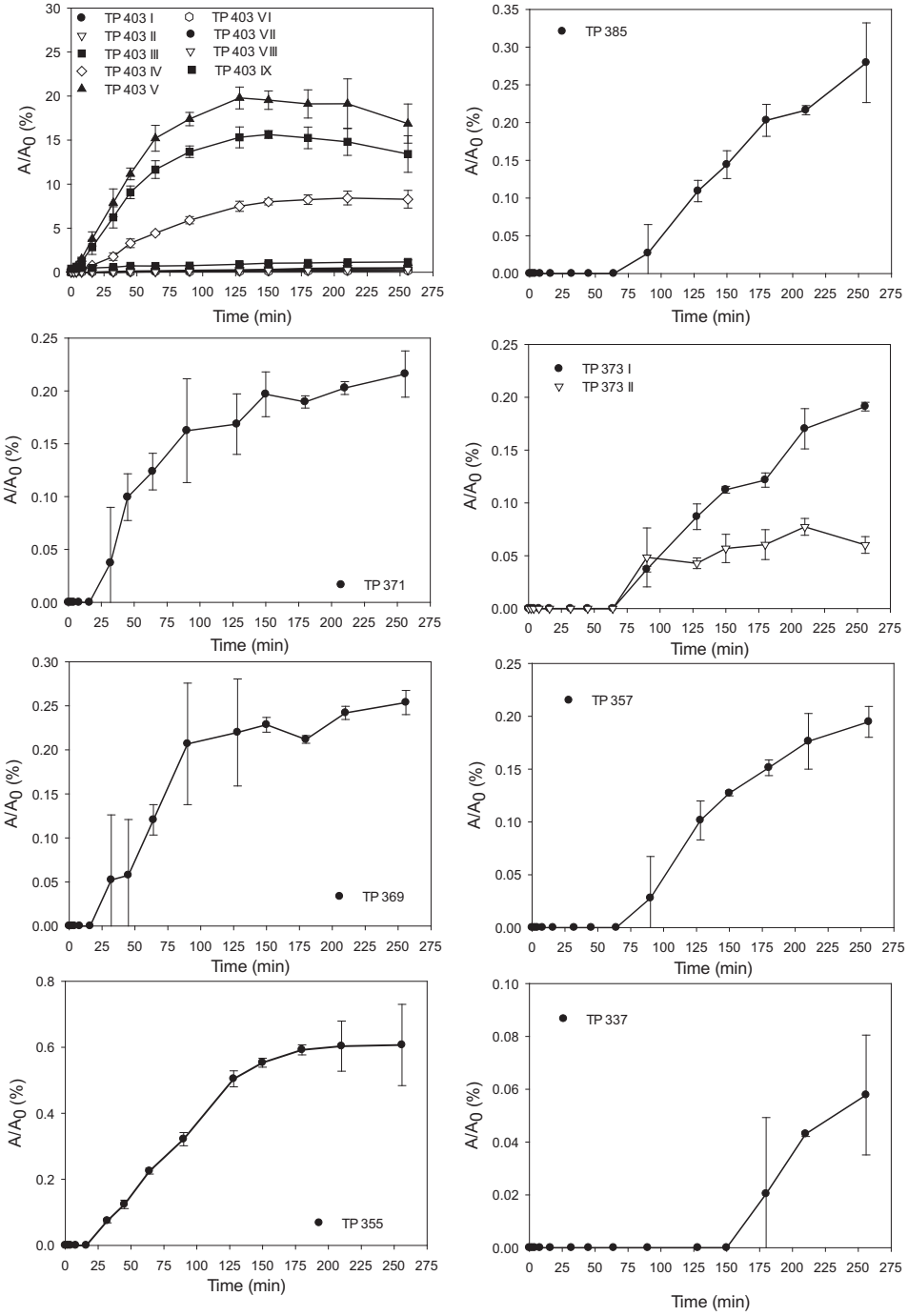

Fig. 4. Profile of the normalized peak area with A/A_0 (%) of the Transformation Products (TPs) during the photolysis by means of Xe lamp (TXE 150 W) irradiation. Data obtained by using the extracted ion chromatogram acquired through LC-HRMS in full scan mode (50–500 *m/z*). Initial conditions: [MESO·besylate] 50 mg L^{-1} (35.48 mg L^{-1} of MESO only), pH 7.0, temp.: 20 ± 2 °C ($n = 2$).

Please cite this article as: Wilde, M.L., et al., Combination of experimental and *in silico* methods for the assessment of the phototransformation products of the antipsychotic drug/metabolite Mesoridazine, Sci Total Environ (2017), https://doi.org/10.1016/j.scitotenv.2017.08.040

The A/A_0 profile of TPs 403 III and V have shown an increase up to 150 min of photolysis followed by a further transformation. The peak area profile of TPs has indicated that the preferential degradation pathway in the beginning of photolysis was through hydroxylation/sulfoxidation, while other TPs were formed later as can be seen in Fig. 4. The TP 371, TP 360, and TP 355 were detected after 16 min of photolysis only, whereas TP 385, TP 373 I and II, and TP 357 were noticed after 64 min of photolysis, and TP 337 only appeared after 150 min of photolysis.

3.3. Aerobic biodegradability of phototransformation products

The validity criteria of CBT and MRT were fulfilled (as for data see Text S9, Supplementary material). Biodegradation of 23.3% and 18.6% was observed in CBT regarding O_2 consumption (*i.e.* biochemical oxygen demand, BOD) for MESO·besylate at 0 min and after 256 min of photolysis, respectively (Table 1). Given the natural variation in the biological CBT test system that is no difference. According to the OECD 301 test series, a substance is considered readily biodegradable if >60% of ThOD is achieved after 28 days of the test (OECD, 1992). Consequently, MESO·besylate has to be classified as not readily biodegradable. In a CBT, which could also be called a BOD_{28} test (biological oxygen demand after 28 days), performed in our laboratory earlier, biodegradation of pure benzenesulfonic acid (besylate) was 25.0% (±5.65%) after 28 days (Fig. S3, Supplementary material). Benzenesulfonic acid showed to be resistant to BOD_5 (20 °C) biodegradation, however bacteria present in raw municipal sewage degraded benzenesulfonic acid after an adaptation period (Janeczko and Gomólka, 1990). Besides, benzenesulfonic acid was found to be biodegradable in the Japanese MITI test (Kawasaki, 1980). Therefore, it can be assumed that the observed biodegradation of MESO·besylate is mainly due to the biodegradation of the besylate counterion itself and MESO is not biodegradable at all.

In the MRT Mesoridazine besylate achieved 6.4% and 0.7% of biodegradation at 0 min and after 256 min of photolysis, respectively (Table 1). That is no significant difference and relates to "not biodegradable". The toxicity control vessels in both tests indicated no toxicity according to the OECD guidelines since >25% of biodegradation was reached in the controls (OECD, 1992).

In order to assess if MESO and TPs undergo any transformation during the biodegradation tests, samples collected during the tests were analyzed by LC-ESI-IT-MS^n. The photo-instability, presence of dissolved oxygen, and autocatalytic characteristics of phenothiazine-derived Pharmaceuticals (Manju et al., 2012; Nałecz-Jawecki et al., 2008) led some TPs of MESO were already present in the sample before photolysis (0 min, Fig. 5 A and 5C).

Fig. 5 (A) shows the peak area results of the CBT. It was found that the peak area of MESO did not decrease throughout the test. Instead, it increased. Back-transformation of TPs to MESO could be an explanation for this since the increase in peak area of MESO goes along with a decrease in peak area of the TPs present in the same sample. The CBT results of the sample collected after 256 min of photolysis and containing at most TPs can be seen in Fig. 5 (B). No significant differences were observed in terms of peak area for the TPs after 28 days of CBT (*i.e.* not biodegradable). MESO was stable in the complex mixture, giving evidence that the biodegradation found in CBT (in terms of BOD) can be attributed to the counterion besylate.

Regarding the EIC peak area results of MRT, which demands a higher inoculum volume, a different behavior was observed for MESO (Fig. 5 (C)). As observed, TPs were again present in this sample, a decrease in peak area of MESO was followed by an increase in the peak area of TPs 403 II and III. The same behavior was also observed in the toxicity control (Text S9, Supplementary material). However, in the sterile control, the EIC peak area results were similar as those found in CBT, MESO presented an increase in peak area, which was followed by a decrease in the peak area of the TPs in this sample (Text S9, Supplementary material).

Fig. 5 (D) depicts the results of the sample taken after 256 min of photolysis and submitted to MRT. The TP 403 V underwent a reduction in peak area after 28 days of the test. No significant changes in peak area were observed for MESO and most of the TPs present this sample were stable during the test. The sterile control showed a reduction in chromatographic peak area for the most of TPs indicating that abiotic processes as described above take place.

MESO has a tricyclic ring and an electron-withdrawing moiety ($S(O)CH_3$) as the R2-substituent group and a hydrophilic side chain as an R1-substituent group. According to the 'rules of thumb' for biodegradation (Boethling et al., 2007) such molecular features do not favor biodegradability. The introduction of an oxygen atom can as hydroxyl group favor aerobic biodegradation (Boethling et al., 2007), which was observed other studies (Rastogi et al., 2015, 2014). The photolysis of MESO led to TPs presenting hydroxylation and sulfoxidation, but biodegradation was not observed in the present study. However, abiotic processes were the main responsible for the reduction in chromatographic peak area, which is in agreement with the biodegradation tests applied to phenothiazine-derived Pharmaceuticals (Trautwein and Kümmerer, 2012a, 2012b; Wilde et al., 2017, 2016).

3.4. Bacterial toxicity of MESO and its photolytic TPs

The concentration-response relationships of MESO in the modified LBT and the parameters of the fitted curves are presented in Text S10 (Supplementary material). The resulting EC_{50} values were 18.1 μmol L^{-1} (30 min) and 25.4 μmol L^{-1} (24 h) for luminescence inhibition and 211.2 μmol L^{-1} for growth inhibition. The measured concentration of MESO and the A/A_0 profile of the TPs in the reaction mixture used for toxicity testing is presented in Fig. 1 (A) (50.00 mg L^{-1} MESO, *i.e.* 70.46 mg L^{-1} of MESO·besylate) and Text S11 (Supplementary material), respectively.

The irradiation of MESO resulted in a moderate reduction of short-term and long-term luminescence inhibition (Figs. 6 (A) and 6 (B)). In both cases, the observed effect of the photolysis mixture was well explained by the predicted effect of MESO over the whole treatment process. In the case of growth inhibition, it was not possible to identify any activity changes during the treatment process, since the observed effect was below the 20% threshold for significance in all tested samples (Fig. 6 (C)). In conclusion, the observed residual effect of the photolytic mixture was most probably caused by MESO alone, which is in agreement with the finding that the mixture of TPs as a whole possessed a considerably lower bacterial toxicity than the parent compound.

Table 1
Results of the investigated aerobic biodegradation test assays applied for Mesoridazine besylate before and after 256 min of photolysis by means of Xe lamp (TXE 150 W) irradiation.

Biodegradation test	Substance	Test sample (min)	Biodegradation after 28 days (%)	Biodegradation in toxicity control after 28 days (%)	Degradation in the sterile control after 28 days (%)	DOC elimination (%)
Closed bottle test	Mesoridazine besylate	0	23.25 (±1.20)	48.10 (±0.62)	–	–
(OECD 301 D)		256	18.60 (±3.20)	45.57	–	–
Manometric respirometry test	Mesoridazine besylate	0	6.39 (±5.42)	43.94	2.67	16.9
(OECD 301 F)		256	0.72 (±2.59)	34.94	1.00	20.4

Please cite this article as: Wilde, M.L., et al., Combination of experimental and *in silico* methods for the assessment of the phototransformation products of the antipsychotic drug/metabolite Mesoridazine, Sci Total Environ (2017), https://doi.org/10.1016/j.scitotenv.2017.08.040

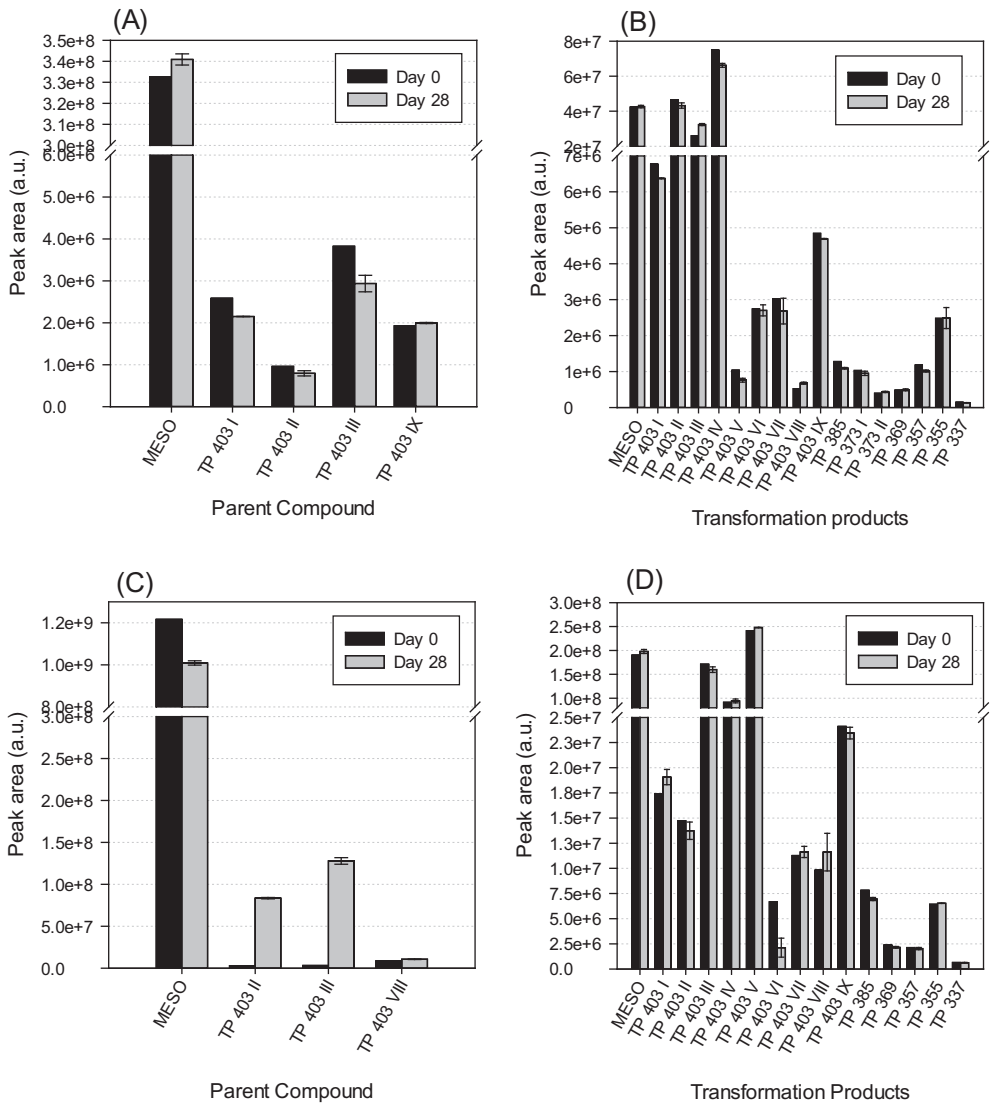

Fig. 5. LC-MS/MS peak areas of Mesoridazine (MESO) and Transformation Products (TPs) before and after 28 days of aerobic biodegradation. (A) Closed Bottle Test of MESO before photolysis (*i.e.* $t = 0$ min); (B) Closed Bottle Test of MESO and TPs after 256 min of photolysis; (C) Manometric Respirometry Test of MESO before photolysis (*i.e.* $t = 0$ min); and (D) Manometric Respirometry Test of MESO and TPs after 256 min of photolysis ($n = 2$).

3.5. Screening of potential PBT/vPvB compounds among the TPs of Mesoridazine

Regarding compounds with known chemical structures but unknown properties and effects, the use of *in silico* QSAR predictions is a valuable tool in their risk assessment. Gramatica et al. (2015) have proposed a consensus among the *in silico* QSAR predictions of US-EPA PBT profiler and the QSARINS Insubria-PBT index regarding the screening of PBT/vPvB compounds. The criteria adopted in both US-EPA PBT profiler and QSARINS Insubria-PBT index can be seen in Text S13 and Text S14 (Supplementary material). With that in mind, we have applied such screening methodology to the TPs formed from the photolysis of MESO in order to identify possible PBT/vPvB compounds among the TPs.

All structures presented values below the QSARINS cutoff value (0.0833) and were in the applicability domain (AD) of the model. The exception was the TP 403 VIII alt, which presented a value higher than the cutoff (0.0928), not being within the AD. Accordingly, the different possible structures of the TPs were submitted to both PBT profiler and QSARINS software using the same classification methodology proposed by Gramatica and co-workers (Cassani and Gramatica, 2015; Gramatica et al., 2015; Sangion and Gramatica, 2016). The *in silico* predictions of US-EPA PBT profiler and QSARINS Insubria-PBT index can be seen in Text S15 (Supplementary material). Fig. 7 presents the results by plotting the US-EPA PBT profiler index *versus* the QSARINS Insubria-PBT index. The QSARINS Insubria-PBT index predictions have been reported as more precautionary than US-EPA PBT index (Gramatica et al., 2015). The TPs are divided into three groups by reference lines (18 for US-EPA PBT profiler and 1.5 for the QSARINS Insubria-PBT index). The group (I) can be classified as non-PBT compounds, once both separated *in silico* QSAR indexes have classified them in this order. The TPs classified in this group were the most of the stereochemical structures of the TPs 403 (I-IX) and TP 373 I, either being the result of hydroxylation or sulfoxidation MESO. TP 403 IX was proposed to be Sulforidazine, a human metabolite of MESO formed in phase I of the metabolic process and as described above is pharmacologically active (Borges et al., 2007). As expected, the sulfoxidation and/or hydroxylation produce an increase in molecule polarity, consequently, decrease the log K_{OW} and log BCF values. Consequently, such TPs are more hydrophilic and would be dispersed in the aquatic environment with no tendency to bioaccumulation.

The group (II) shows the TPs which were classified as PBT compounds by US-EPA PBT profiler but not by the *in silico* predictions of QSARINS Insubria-PBT index. This could be overestimated PBT compounds according to Gramatica et al. (2015). The parent compound

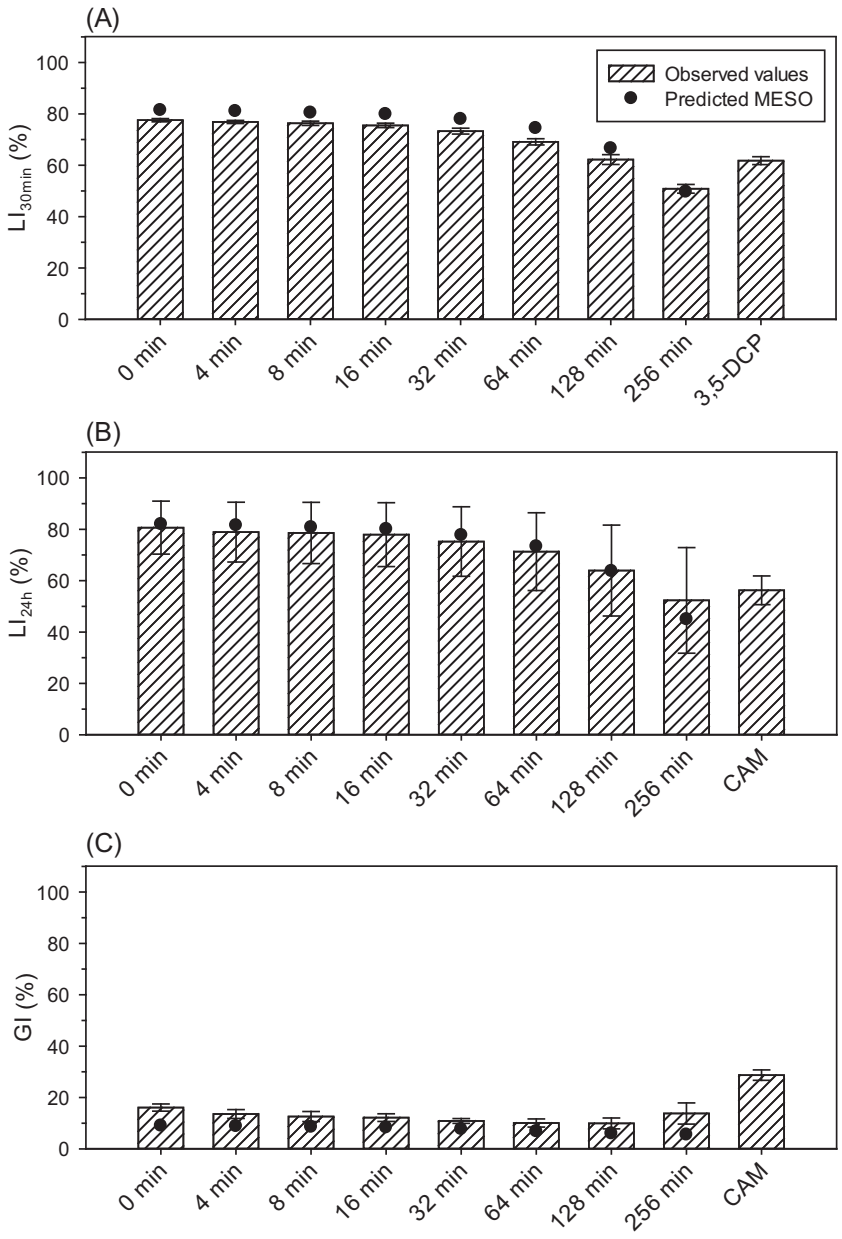

Fig. 6. Observed effect values (mean ± SD) of the photolytic mixture of 129.3 μmol L^{-1} Mesoridazine besylate (MESO) in comparison to the predicted effect of residual MESO by means of short-term luminescence inhibition after 30 min (A), long-term luminescence inhibition after 24 h (B) and growth inhibition (C) in the modified luminescent bacteria test. The positive control samples contained 9 mg L^{-1} of 3,5-Dichlorophenol (3,5-DCP) and 0.2 mg L^{-1} Chloramphenicol (CAM). The final concentration in the test medium of the photolytic mixture and the positive control samples was 50% (*v*/v).

MESO and TPs in this group resulted from dehydroxylation (TP 371, Thioridazine), dehydrogenation (TP 385), both dehydroxylation and dehydrogenation (TP 369), demethylation (TP 373 II) and even the hydroxylated variants from TP 403 (VI, VIII) with OH attachment at the C1- and C9-position of the phenothiazine moiety. The predictions of PBT profiler for TP 403 VI and VIII provided higher values for log K_{OW}, log BCF and lower values for toxicity (Fish Ch.V.) regarding the hydroxylation on C1- and C9-position of the phenothiazine ring. On the other hand, QSARINS Insubria-PBT index values for these TPs indicated no considerable difference among the possible different positions where the hydroxylation could take place on the phenothiazine tricycle ring.

The group (III) in Fig. 7 contain TP 337 and TP 355 being PBT compounds according to both indexes and can be considered as PBT/vPvB compounds in a consensus mode (*i.e.* both indexes (QSARINS Insubria-PBT index and US-EPA PBT index agreed in the predictions). These two TPs are carbazole derivatives. TP 355 and TP 337 were formed in lower A/A_0 ratio and after 16 min and 150 min of photolysis, respectively. The profile of A/A_0 (see Fig. 4) indicates that these TPs show a tendency to increase with longer exposition times, which is in agreement with the observation of Manju et al. (2012). Moreover, carbazole-derived TPs have also been reported as TPs from the degradation of diclofenac (Musa and Eriksson, 2009; Salgado et al., 2013). Although not the same compounds as the carbazole derivative TPs found in this study, halogenated derived carbazoles have shown persistence and dioxin-like toxicity in soil (Mumbo et al., 2014), providing an indication of the PBT potential of carbazole derivatives. Therefore, a more prominent assessment of the carbazole derivative TPs should be further considered.

3.6. QSAR predictions of genotoxicity and mutagenicity

The *in silico* QSAR predictions considering all structures of the proposed TPs including possible isomers are given in Table 2. SMILES of

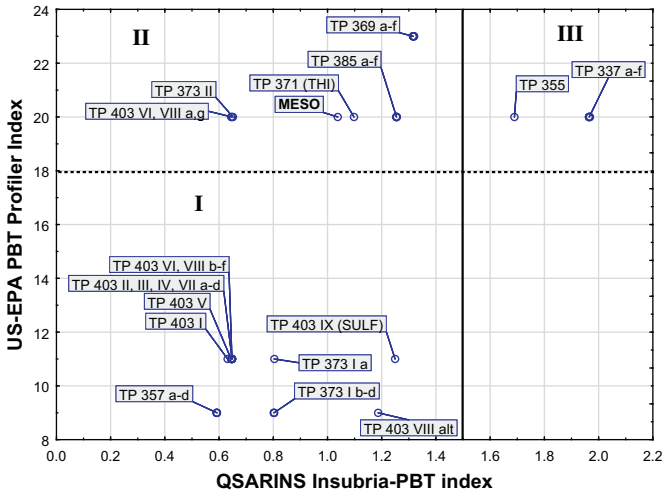

Fig. 7. The plot of US EPA PBT profiler index *versus* QSARIN Insubria-PBT index for the identification of potential PBT/vPvB compounds among the TPs formed from MESO by photolysis.

all structures proposed can be seen in Text S12 (Supplementary material). MESO and most of the TPs formed have been classified as "inconclusive", "out of domain" and "negative" alerts. The "inconclusive" alert means that the calculated probability of the proposed structure being positive falls inside the so-called "gray zone", which depends on the model applied, whereas "out of domain" means that the structure tested is not covered by the applicability domain of the applied QSAR model. The "negative" alerts point out that that the analyzed structure has a calculated probability of being positive lower than the model's classification threshold (50.0%) and is not within the "gray zone". In other words, predicted negative alerts indicate that the compounds are classified as not presenting genotoxicity and mutagenic activities according to their molecular structure. On the other hand, "positive" alerts indicate that the probability of the tested structure being positive as for the endpoint tested is higher than the model's classification threshold (50.0%) and is not within the "gray zone".

The "Konsolidator" (column F in Table 2) is a tool of the CASE Ultra software intended to generate evidence for review and regulatory issues by combining and re-evaluating the multiple statistical and expert rule models. The "Konsolidator" considers the following features: (i) It is based on the multiple statistical and expert rule models; (ii) It compares the tested compounds with active pharmaceuticals ingredients (API) or inert compounds; (iii) Comprehensive literature reference in support of the data is provided; (iv) Automatic neighborhood analysis of the tested compound is performed; (v) Evaluates the alerts and their validity; (vi) Assesses unknown fragments; and (vii) Increase in the coverage of the *in silico* predictions by resolving "out of domain" and "inconclusive" alerts is provided.

Based on the "Konsolidator" features, MESO and most of TPs were classified as presenting negative predictions for bacterial mutagenicity as can be observed in Table 2. However, two TPs, namely TP 355 and TP 337, presented statistically and rule-based positive alerts for mutagenicity in bacteria according to the CASE Ultra models applied, indicating that these TPs might have structural features closely linked to DNA-reactivity. Positive prediction for bacterial mutagenesis towards *Salmonella typhimurium* was also pointed out by Leadscope Model Applier models. Additionally, the Leadscope software has pointed out negative predictions for MESO and the most of TPs proposed in the Mammalian mutation model. The same trend was also observed the Leadscope models regarding the genotoxic activities of the models *in vitro* chromosome aberrations average model and *in vivo* Micronucleus single model.

TP 355 and TP 337 are carbazole derivatives TPs. Fig. 8 depicts the formation of the carbazole tricyclic ring according to Manju et al. (2012), and highlight the structural alerts (in bold) for bacterial mutagenicity provided by the CASE Ultra models. TP 355 and all possible different structures proposed for TP 337 have the same structural alerts with high statistical significance, which is because of the shared carbazole backbone.

The predicted mutagenic activity of carbazole derivatives is supported by experimental results. Carbazole derivatives might have caused

Table 2
In silico QSAR predictions for mutagenicity of Mesoridazine and all possible different structures proposed for the TPs formed during photolysis according to QSAR models provided by Multicase CASE Ultra™ and Leadscope Model Applier™ (A-J: Software models used, as for details see at the end of the table).

Structure ID[a]	QSAR predictions									
	Case Ultra[b]						Leadscope[c]			
	A	B	C	D	E	F	G	H	I	J
Mesoridazine	IN	−	−	−	−	−	−	−	−	−
TP 403 I	IN	OD	−	OD	−	−	−	−	−	−
TP 403 II, III, IV, VII a	IN	−	−	−	−	−	−	−	OD	−
TP 403 II, III, IV, VII b	IN	−	−	−	−	−	−	−	OD	−
TP 403 II, III, IV, VII c	IN	−	−	−	−	−	−	−	−	−
TP 403 II, III, IV, VII d	IN	OD	−	OD	−	−	−	−	OD	−
TP 403 V	IN	−	−	−	−	−	−	−	OD	−
TP 403 VI, VIII a	IN	−	−	−	−	−	−	−	OD	−
TP 403 VI, VIII b	IN	−	−	−	−	−	−	−	OD	−
TP 403 VI, VIII c	IN	−	−	−	−	−	−	−	OD	−
TP 403 VI, VIII d	IN	−	−	−	−	−	−	−	OD	−
TP 403 VI, VIII e	−	−	−	−	−	−	−	−	OD	−
TP 403 VI, VIII f	OD	OD	−	−	−	−	−	−	OD	−
TP 403 VI, VIII g	IN	OD	−	−	−	−	−	−	OD	−
TP 403 IX	IN	−	−	−	−	−	−	−	−	−
TP 403 VIII alt	OD	OD	−	OD	−	−	−	−	OD	−
TP 373 I a	−	OD	−	−	−	−	OD	OD	OD	OD
TP 373 I b	−	OD	−	−	−	−	OD	OD	OD	−
TP 373 I c	−	OD	−	−	−	−	OD	OD	OD	OD
TP 373 I d	−	OD	−	−	−	−	OD	OD	OD	−
TP 373 II	IN	−	−	−	−	−	−	−	−	−
TP 371 (Thioridazine)	IN	−	−	−	−	−	−	−	−	−
TP 385 a	IN	−	−	−	−	−	−	−	−	−
TP 385 b	IN	OD	−	−	−	−	−	−	−	−
TP 385 c	IN	OD	−	−	−	−	−	−	−	−
TP 385 d	IN	−	−	−	−	−	−	−	−	−
TP 385 e	IN	OD	−	−	−	−	−	−	−	−
TP 385 f	IN	OD	−	−	−	−	−	−	−	−
TP 369 a	IN	−	−	−	−	−	−	−	−	−
TP 369 b	IN	OD	−	−	−	−	−	−	−	−
TP 369 c	IN	OD	−	−	−	−	−	−	−	−
TP 369 d	IN	−	−	−	−	−	−	−	−	−
TP 369 e	IN	OD	−	−	−	−	−	−	−	−
TP 369 f	IN	OD	−	−	−	−	−	−	−	−
TP 357 a	OD	OD	−	OD	−	−	OD	OD	OD	−
TP 357 b	OD	OD	−	OD	−	−	OD	OD	OD	−
TP 357 c	OD	OD	−	OD	−	−	OD	OD	OD	OD
TP 357 d	OD	OD	−	OD	−	−	OD	OD	OD	−
TP 355	+	+	+	+	+	+	−	OD	OD	+
TP 337 a	+	+	+	+	+	+	−	OD	OD	+
TP 337 b	+	+	+	+	+	+	−	OD	OD	+
TP 337 c	+	+	+	+	+	+	−	OD	OD	+
TP 337 d	+	+	+	+	+	+	−	OD	OD	+
TP 337 e	+	+	+	+	+	+	−	OD	OD	+
TP 337 f	+	+	+	+	+	+	OD	OD	OD	OD

OD (Out of Domain): tested chemical is not covered by the applicability domain of the model.
IN (Inconclusive): the calculated probability of being positive falls inside the "gray zone" (35%–65% of probability for A and 40%–60% of probability for B, C, D, and E).
(+) positive alert (>60%). (−) negative alert (<40%).

[a] The SMILES codes of the structure ID of the TPs can be seen in Text S12 (Supplementary material). The letters represent different isomers of TPs with the same *m/z* (*i.e.* OH or double bond position).

[b] Case Ultra models according to ICH guideline M7: (A) GT1_A7B (*Salmonella t.* 7-strains (RCA)); (B) GT1_AT_ECOLI (*E. coli/Salmonella* TA102 (A-T Base Pair Mutation)); (C) GT_EXPERT (Expert Rules for Bacterial Mutagenicity); (D) PHARM_ECOLI (*E.coli* mutagenicity (all strains)); (E) PHARM_SALM (*Salmonella* mutagenicity (TA97,98,100,1535-1538)); (F) "Konsolidator" Outcome.

[c] Leadscope models: (G) *In Vitro* Chromosome aberrations average model; (H) Mammalian mutation; (I) *In vivo* Micronucleus single model; (J) Bacterial mutagenesis towards *Salmonella typhimurium*.

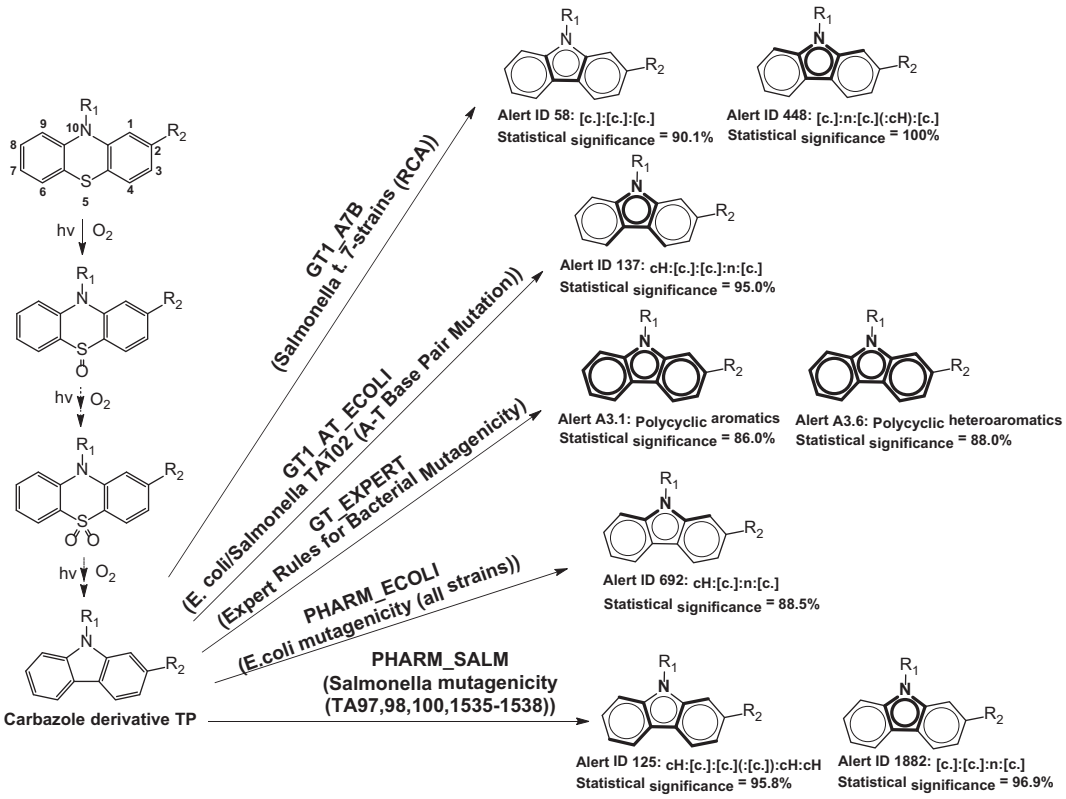

Fig. 8. Formation of a carbazole ring through photolysis (adapted from Manju et al., 2012) and the structural alerts (in bold) responsible for the positive alerts in the carbazole tricyclic ring of TP 355 and TP 337 provided by CASE Ultra software according to the ICH M7 guideline.

DNA mutation in a male germ cell of Swiss albino mice (Jha and Bharti, 2002), and some methyl-, nitro- and amino-substituted carbazoles were found to be mutagenic to *Salmonella typhimurium* (André et al., 1997, 1995; Grover and Bala, 1993; LaVoie et al., 1982). One of the molecular descriptors that are correlated to the mutagenic activity of carbazole derivatives is the hydrophobicity (André et al., 1997).

3.7. Environmental significance and implications

The isolation and/or synthesis of so many TPs to allow separately tests for an extended assessment is impracticable for financial reasons. Thus, this study aimed to better understand the significance of the TPs formed and present a workflow how this can be done. The screening approach as presented in the paper helps to resolve this issue as it allows for collecting basic information and the selection of compounds being of most interest for a PBT/vPvB assessment thereby allowing including TPs in such an assessment. The use of high initial concentrations enables to generate a broad range of TPs at levels that would allow an analytical detection and studying biodegradability as well as toxicity experimentally for proactive assessment of fate and effects. Especially because of the sunlight simulating photolysis has been shown to be a mere phototransformation process (Wang and Lin, 2014). Photo TPs are of interest if they are not biodegradable in the environment. The use of environmentally relevant concentrations would make these tests unfeasible, due to the high ThOD required for such tests. However, biodegradability is an important parameter for environmental risk assessment as well as for sustainability and green chemistry, once the development of new pharmaceuticals compounds should focus on their biodegradability, minimizing the exposure of ecosystems and, consequently, humans to pharmaceuticals (Kümmerer, 2007; Leder et al., 2015; Rastogi et al., 2015).

In comparison to the photolysis of Thioridazine (Wilde et al., 2016), an active pharmaceutical ingredient precursor of MESO in the human body, the photolysis of the human metabolite MESO produced a similar kind of TPs as Thioridazine, but in less number and with structural differences due to the different precursor compounds. The same kind of mechanism was verified for both compounds by means of Xe lamp (TXE 150 W) irradiation. This also shows that the same TPs can evolve from the degradation of different compounds. New TPs were found as well, consequently, this new mixture of TPs was further analyzed in aerobic biodegradability tests and as for toxicity. Consequently, an isolated assessment of related APIs may underestimate the true risk of common TPs.

The evidence of photolytic back-transformation from MESO to Thioridazine by means of Xe lamp (TXE 150 W) irradiation in this manuscript provides evidence that photolysis through natural sunlight might not entirely attenuate the presence of the parent drugs in the environment, but to some extent even may regenerate them. This might be especially important in cases where the metabolite shows a much lower pharmacological or toxicological activity than its precursor parent drug. As an example, Thioridazine was determined to be approximately 18-fold more active than MESO regarding the inhibition of bacterial growth (Wilde et al., 2016). Therefore, research on the contribution of natural abiotic process on human metabolites and TPs as a possible back-transformation process should be further investigated.

The high initial concentration of MESO allowed for the experimental study of the ready biodegradability by applying two OECD standardized tests, CBT (OECD 301D) and MRT (OECD 301F), which have indicated that MESO and the mixture of its photo TPs are not biodegradable. That implies that they persist in the environment as they are stable end products of photolysis too. The decrease in concentration of MESO and the formation of hydroxylated and sulfoxide as the main TPs had led to a decrease in the ecotoxicity towards *V. fischeri*. However, psychiatric drugs might alter the composition of freshwater invertebrate communities, as was the case of carbamazepine (Jarvis et al., 2014a, 2014b).

The pressure for identification of possible hazardous compounds and their substitution for greener (*i.e.* safer) ones is urgently needed (Alves et al., 2016). The identification of possible hazardous TPs is a

necessity in this context. The combination of experimental work and *in silico* QSAR models had proved to be a powerful screening approach in the risk assessment of unknown compounds such as TPs as demonstrated in this study allows for a better understanding of environmental risks and even to further prioritize possibly hazardous compounds for further testing. Concerning the TPs of MESO found in this study, attention should be given to the formation of carbazole derivatives by photolysis indicated as possible mutagenic and putative PBT/vPvB according to QSAR *in silico* predictions and literature related to other carbazole derivatives that were observed in the photolysis of both compounds, Thioridazine (Wilde et al., 2016) and MESO.

4. Conclusions

The photolysis of the antipsychotic and drug metabolite MESO through Xe lamp irradiation led to a series of TPs. Sixteen TPs were proposed according to LC-HRMS^n and, among them, abiotic back-transformation from MESO to Thioridazine was observed, indicating that natural attenuation of metabolites could also contribute to the environmental exposition of the parent compounds. Besides, the photolysis of MESO led to new chiral TPs. Chiral compounds might possess different pharmacological activities and toxicities, needing further investigations. No ready biodegradability of the parent compound was observed in CBT and MRT neither for the photo-TPs was observed. A reduction in toxicity towards *V. fischeri* during photolysis was mainly related to MESO's decline in concentration. *In silico* predictions of QSARINS and US-EPA PBT profiler pointed out TP 355 and TP 337 as PBT/vPvB compounds in a consensus mode. Likewise, statistical and rule-based *in silico* predictions for mutagenicity and genotoxicity indicated positive alerts for bacterial mutagenicity in TP 355 and TP 337. Therefore, this study strongly indicates a possible hazard associated with the two carbazoles derivative TPs, calling for further investigations on such derivatives to confirm their hazardous alerts experimentally.

The combination of experimental and *in silico* tools allowed studying MESO and TPs as a starting point to better understand the environmental fate and effects of metabolic compounds. Besides, future studies should focus beyond the parent compounds and more attention should be given to metabolites and their TPs. A screening study and a workflow for the assessment of photoproducts combining experimental and *in silico* work was performed allowing to get new insights and include knowledge about TPs of a pharmaceutical present in the environment and their PBT relevant properties.

Acknowledgments

The authors would like to thank the Brazilian program “Science without borders” from CNPq/CAPES/CsF (Grant Nr. 2367712012-4) and the Innovations-Inkubator Lüneburg (Teilmaßnahme 1.4, Graduate School) for the scholarships granted to Dr. M.L. Wilde and J. Menz, respectively. The authors would like to thank A. Haiss and E. Logunova for planning the aerobic biodegradation tests and S. Hinz for helping in the toxicity test. Multicase Inc. and Leadscope Inc. are kindly acknowledged for providing the CASE Ultra and Leadscope QSAR programs, respectively. Dr. P. Gramatica is acknowledged for providing the QSARINS software (www.qsar.it).

Conflicts of interest

The authors declared to have no conflict of interest.

Appendix A. Supplementary data

Supplementary data to this article can be found online at https://doi.org/10.1016/j.scitotenv.2017.08.040.

References

Alagarsamy, V., 2010. Textbook of Medicinal Chemistry. 1st ed. Elsevier India, New Delhi, India.

Alves, V.M., Muratov, E.N., Capuzzi, S.J., Politi, R., Low, Y., Braga, R.C., Zakharov, A.V., Sedykh, A., Mokshyna, E., Farag, S., Andrade, C.H., Kuz'min, V.E., Fourches, D., Tropsha, A., 2016. Alarms about structural alerts. Green Chem. 18:4348–4360. https://doi.org/10.1039/C6GC01492E.

Amaral, L., 2012. Thioridazine: an old neuroleptic effective against totally drug resistant tuberculosis. Acta Medica Port. 25, 118–121.

André, V., Boissart, C., Sichel, F., Gauduchon, P., Le Talaër, J.Y., Lancelot, J.C., Robba, M., Mercier, C., Chemtob, S., Raoult, E., Tallec, A., 1995. Mutagenicity of nitro- and amino-substituted carbazoles in Salmonella typhimurium. II. Ortho-aminonitro derivatives of 9H-carbazole. Mutat. Res. 345:11–25. https://doi.org/10.1016/0165-1218(95)90066-7.

André, V., Boissart, C., Sichel, F., Gauduchon, P., Le Talaër, J.Y., Lancelot, J.C., Mercier, C., Chemtob, S., Raoult, E., Tallec, A., 1997. Mutagenicity of nitro- and amino-substituted carbazoles in *Salmonella typhimurium*. III. Methylated derivatives of 9H-carbazole. Mutat. Res. 389:247–260. https://doi.org/10.1016/S1383-5718(96)00155-6.

Boethling, R.S., Sommer, E., DiFiore, D., 2007. Designing small molecules for biodegradability. Chem. Rev. 107:2207–2227. https://doi.org/10.1021/cr050952t.

Bonvin, F., Omlin, J., Rutler, R., Schweizer, W.B., Alaimo, P.J., Strathmann, T.J., McNeill, K., Kohn, T., 2013. Direct photolysis of human metabolites of the antibiotic sulfamethoxazole: evidence for abiotic back-transformation. Environ. Sci. Technol. 47:6746–6755. https://doi.org/10.1021/es303777k.

Borges, K.B., Borges, W.D.S., Pupo, M.T., Bonato, P.S., 2007. Endophytic fungi as models for the stereoselective biotransformation of thioridazine. Appl. Microbiol. Biotechnol. 77: 669–674. https://doi.org/10.1007/s00253-007-1171-x.

Cassani, S., Gramatica, P., 2015. Identification of potential PBT behavior of personal care products by structural approaches. Sustain. Chem. Pharm. 1:19–27. https://doi.org/10.1016/j.scp.2015.10.002.

Celiz, M.D., Tso, J., Aga, D.S., 2009. Pharmaceutical metabolites in the environment: analytical challenges and ecological risks. Environ. Toxicol. Chem. 28:2473–2484. https://doi.org/10.1897/09-173.1.

Chakravarti, S.K., Saiakhov, R.D., Klopman, G., 2012. Optimizing predictive performance of CASE Ultra expert system models using the applicability domains of individual toxicity alerts. J. Chem. Inf. Model. 52:2609–2618. https://doi.org/10.1021/ci300111r.

Chen, Y., Hu, C., Qu, J., Yang, M., 2008. Photodegradation of tetracycline and formation of reactive oxygen species in aqueous tetracycline solution under simulated sunlight irradiation. J. Photochem. Photobiol. A Chem. 197:81–87. https://doi.org/10.1016/j.jphotochem.2007.12.007.

Choi, S., Haggart, D., Toll, L., Cuny, G.D., 2004. Synthesis, receptor binding and functional studies of mesoridazine stereoisomers. Bioorg. Med. Chem. Lett. 14:4379–4382. https://doi.org/10.1016/j.bmcl.2004.06.078.

Cwiertny, D.M., Snyder, S.A., Schlenk, D., Kolodziej, E.P., 2014. Environmental designer drugs: when transformation may not eliminate risk. Environ. Sci. Technol. 48, 11737–11745.

De Gaitani, C.M., Martinez, A.S., Bonato, P.S., 2004. Degradation and configurational changes of thioridazine 2-sulfoxide. J. Pharm. Biomed. Anal. 36:601–607. https://doi.org/10.1016/j.jpba.2004.07.011.

Du, Y., Chen, H., Zhang, Y., Chang, Y., 2014. Photodegradation of gallic acid under UV irradiation: insights regarding the pH effect on direct photolysis and the ROS oxidation-sensitized process of DOM. Chemosphere 99:254–260. https://doi.org/10.1016/j.chemosphere.2013.10.093.

Eap, C.B., Guentert, T.W., Schäublin-Loidl, M., Stabl, M., Koeb, L., Powell, K., Baumann, P., 1996. Plasma levels of the enantiomers of thioridazine, thioridazine 2-sulfoxide, thioridazine 2-sulfone, and thioridazine 5-sulfoxide in poor and extensive metabolizers of dextromethorphan and mephenytoin. Clin. Pharmacol. Ther. 59:322–331. https://doi.org/10.1016/S0009-9236(96)80010-5.

Edhlund, B.L., Arnold, W.A., McNeill, K., 2006. Aquatic photochemistry of nitrofuran antibiotics. Environ. Sci. Technol. 40:5422–5427. https://doi.org/10.1021/es0606778.

Eiduson, S., Geller, E., 1963. The excretion and metabolism of ^{35}S-labeled thioridazine in urine, blood, bile, and feces. Biochem. Pharmacol. 12, 1429–1435.

Faria, P.A., Bettanin, F., Cunha, R.L.O.R., Paredes-Gamero, E.J., Homem-de-Mello, P., Nantes, I.L., Rodrigues, T., 2015. Cytotoxicity of phenothiazine derivatives associated with mitochondrial dysfunction: a structure-activity investigation. Toxicology 330:44–54. https://doi.org/10.1016/j.tox.2015.02.004.

Fasnacht, M.P., Blough, N.V., 2002. Aqueous photodegradation of polycyclic aromatic hydrocarbons. Environ. Sci. Technol. 36:4364–4369. https://doi.org/10.1021/es025603k.

Fatta-Kassinos, D., Vasquez, M.I., Kümmerer, K., 2011. Transformation products of pharmaceuticals in surface waters and wastewater formed during photolysis and advanced oxidation processes — degradation, elucidation of byproducts and assessment of their biological potency. Chemosphere 85:693–709. https://doi.org/10.1016/j.chemosphere.2011.06.082.

Friedrich, J., Längin, A., Kümmerer, K., 2013. Comparison of an electrochemical and luminescence-based oxygen measuring system for use in the biodegradability testing according to closed bottle test (OECD 301D). CLEAN 41:251–257. https://doi.org/10.1002/clen.201100558.

Fura, A., 2006. Role of pharmacologically active metabolites in drug discovery and development. Drug Discov. Today 11:133–142. https://doi.org/10.1016/S1359-6446(05)03681-0.

Gramatica, P., Chirico, N., Papa, E., Cassani, S., Kovarich, S., 2013. QSARINS: a new software for the development, analysis, and validation of QSAR MLR models. J. Comput. Chem. 34:2121–2132. https://doi.org/10.1002/jcc.23361.

Gramatica, P., Cassani, S., Chirico, N., 2014. QSARINS-chem: Insubria datasets and new QSAR/QSPR models for environmental pollutants in QSARINS. J. Comput. Chem. 35: 1036–1044. https://doi.org/10.1002/jcc.23576.

Gramatica, P., Cassani, S., Sangion, A., 2015. PBT assessment and prioritization by PBT index and consensus modeling: comparison of screening results from structural models. Environ. Int. 77:25–34. https://doi.org/10.1016/j.envint.2014.12.012.

Grover, I.S., Bala, S., 1993. Mutagenicity of nitro- and amino-substituted carbazoles in Salmonella typhimurium. I. Monosubstituted derivatives of 9H-carbazole. Mutat. Res. 299:63–73. https://doi.org/10.1016/0165-1218(93)90120-3.

Hawesx, M., 1993. The metabolism of piperidine-type phenothiazine antipsychotic agents. III. Mesoridazine in dog, human and rat. Xenobiotica 23. https://doi.org/10.3109/00498259309059360.

Herrmann, M., Menz, J., Olsson, O., Kümmerer, K., 2015. Identification of phototransformation products of the antiepileptic drug gabapentin: biodegradability and initial assessment of toxicity. Water Res. 85, 11–21.

International Conference on Harmonization (ICH), 2014. ICH guideline M7. http://www.ich.org/fileadmin/Public_Web_Site/ICH_Products/Guidelines/Multidisciplinary/M7/M7_Step_4.pdf, Accessed date: 11 February 2015.

Jacobs, L.E., Weavers, L.K., Houtz, E.F., Chin, Y.-P., 2012. Photosensitized degradation of caffeine: role of fulvic acids and nitrate. Chemosphere 86:124–129. https://doi.org/10.1016/j.chemosphere.2011.09.052.

Janeczko, A., Gomólka, E., 1990. Respirometric investigations on the biodegradability of phenylsulphonic acid. Acta Hydrochim. Hydrobiol. 18:581–590. https://doi.org/10.1002/aheh.19900180511.

Jarvis, A.L., Bernot, M.J., Bernot, R.J., 2014a. Relationships between the psychiatric drug carbamazepine and freshwater macroinvertebrate community structure. Sci. Total Environ. 496:499–509. https://doi.org/10.1016/j.scitotenv.2014.07.086.

Jarvis, A.L., Bernot, M.J., Bernot, R.J., 2014b. The effects of the psychiatric drug carbamazepine on freshwater invertebrate communities and ecosystem dynamics. Sci. Total Environ. 496:499–509. https://doi.org/10.1016/j.scitotenv.2014.07.086.

Jaszczyszyn, A., Gasiorowski, K., SwiaTek, P., Malinka, W., Cieslik-Boczula, K., Petrus, J., Czarnik-Matusewicz, B., 2012. Chemical structure of phenothiazines and their biological activity. Pharmacol. Rep. 64:16–23. https://doi.org/10.1016/S1734-1140(12)70726-0.

Jha, A.M., Bharti, M.K., 2002. Mutagenic profiles of carbazole in the male germ cells of Swiss albino mice. Mutat. Res. 500:97–101. https://doi.org/10.1016/S0027-5107(01)00303-7.

Jin, H.-E., Lee, K.-R., Kang, I.-H., Chung, S.-J., Shim, C.-K., 2014. Determination of mesoridazine by liquid chromatography–tandem mass spectrometry and its application to pharmacokinetic study in rats. J. Chromatogr. B 958:117–123. https://doi.org/10.1016/j.jpba.2010.11.001.

Kasprzyk-Hordern, B., 2010. Pharmacologically active compounds in the environment and their chirality. Chem. Soc. Rev. 39:4466–4503. https://doi.org/10.1039/c000408c.

Kawasaki, M., 1980. Experiences with the test scheme under the chemical control law of Japan: an approach to structure-activity correlations. Ecotoxicol. Environ. Saf. 4: 444–454. https://doi.org/10.1016/0147-6513(80)90046-9.

Kelly, M.M., Arnold, W.A., 2012. Direct and indirect photolysis of the phytoestrogens genistein and daidzein. Environ. Sci. Technol. 46:5396–5403. https://doi.org/10.1021/es300041f.

Kümmerer, K., 2007. Sustainable from the very beginning: rational design of molecules by life cycle engineering as an important approach for green pharmacy and green chemistry. Green Chem. 9:899. https://doi.org/10.1039/b618298b.

Kümmerer, K., 2009. The presence of pharmaceuticals in the environment due to human use — present knowledge and future challenges. J. Environ. Manag. 90:2354–2366. https://doi.org/10.1016/j.jenvman.2009.01.023.

Kümmerer, K., 2010. Pharmaceuticals in the environment. Annu. Rev. Environ. Resour. 35: 57–75. https://doi.org/10.1146/annurev-environ-052809-161223.

Langford, K., Thomas, K.V., 2011. Input of selected human pharmaceutical metabolites into the Norwegian aquatic environment. J. Environ. Monit. 13:416–421. https://doi.org/10.1039/c0em00342e.

LaVoie, E.J., Briggs, G., Bedenko, V., Hoffmann, D., 1982. Mutagenicity of substituted carbazoles in Salmonella typhimurium. Mutat. Res. Toxicol. 101:141–150. https://doi.org/10.1016/0165-1218(82)90004-0.

Leder, C., Rastogi, T., Kümmerer, K., 2015. Putting benign by design into practice-novel concepts for green and sustainable pharmacy: designing green drug derivatives by non-targeted synthesis and screening for biodegradability. Sustain. Chem. Pharm. 2: 1–6. https://doi.org/10.1016/j.scp.2015.07.001.

Leonard, B.E., 2003. Fundamentals of Psychopharmacology. 3rd Ed. WILEY-VCH, Verlag GmbH.

Li, Y., Chen, J., Qiao, X., Zhang, H., Zhang, Y.-nan, Zhou, C., 2016. Insights into photolytic mechanism of sulfapyridine induced by triplet-excited dissolved organic matter. Chemosphere 147:305–310. https://doi.org/10.1016/j.chemosphere.2015.12.115.

Lin, A.Y.-C., Wang, X.-H., Lee, W.-N., 2013. Phototransformation determines the fate of 5-fluorouracil and cyclophosphamide in natural surface waters. Environ. Sci. Technol. 47:4104–4112. https://doi.org/10.1021/es304976q.

López-Serna, R., Jurado, A., Vázquez-Suñé, E., Carrera, J., Petrović, M., Barceló, D., 2013. Occurrence of 95 pharmaceuticals and transformation products in urban groundwaters underlying the metropolis of Barcelona, Spain. Environ. Pollut. 174:305–315. https://doi.org/10.1016/j.envpol.2012.11.022.

Mahmoud, W.M.M., Toolaram, A.P., Menz, J., Leder, C., Schneider, M., Kümmerer, K., 2014. Identification of phototransformation products of thalidomide and mixture toxicity assessment: an experimental and quantitative structural activity relationships (QSAR) approach. Water Res. 49:11–22. https://doi.org/10.1016/j.watres.2013.11.014.

Manju, T., Manoj, N., Braun, A.M., Oliveros, E., 2012. Self-sensitized photooxidation of N-methyl phenothiazine: acidity control of the competition between electron and energy transfer mechanisms. Photochem. Photobiol. Sci. 1744. https://doi.org/10.1039/c2pp25244a.

Menz, J., Schneider, M., Kümmerer, K., 2013. Toxicity testing with luminescent bacteria — characterization of an automated method for the combined assessment of acute and chronic effects. Chemosphere 93:990–996. https://doi.org/10.1016/j.chemosphere.2013.05.067.

Mumbo, J., Henkelmann, B., Abdelaziz, A., Pfister, G., Nguyen, N., Schroll, R., Munch, J.C., Schramm, K.W., 2014. Persistence and dioxin-like toxicity of carbazole and chlorocarbazoles in soil. Environ. Sci. Pollut. Res. 22:1344–1356. https://doi.org/10.1007/s11356-014-3386-6.

Musa, K.A.K., Eriksson, L.A., 2009. Photodegradation mechanism of the common non-steroid anti-inflammatory drug diclofenac and its carbazole photoproduct. Phys. Chem. Chem. Phys. 11:4601–4610. https://doi.org/10.1039/b900144a.

Nałecz-Jawecki, G., Hajnas, A., Sawicki, J., 2008. Photodegradation and phototoxicity of thioridazine and chlorpromazine evaluated with chemical analysis and aquatic organisms. Ecotoxicology 17:13–20. https://doi.org/10.1007/s10646-007-0171-z.

Obach, R.S., 2013. Pharmacologically active drug metabolites: impact on drug discovery and pharmacotherapy. Pharmacol. Rev. 65:578–640. https://doi.org/10.1124/pr.111.005439.

OECD, 1992. Organisation for Economic Co-operation and Development, 2006. OECD Guideline for Testing of Chemicals 301: Ready Biodegradability. OECD Publishing, Paris.

Oppenländer, T., 2003. Photochemical Purification of Water and Air. WILEY-VCH Verlag GmbH & Co. KGaA, Weinheim, Germany.

Osorio, V., Imbert-Bouchard, M., Zonja, B., Abad, J.L., Pérez, S., Barceló, D., 2014. Simultaneous determination of diclofenac, its human metabolites and microbial nitration/nitrosation transformation products in wastewaters by liquid chromatography/quadrupole-linear ion trap mass spectrometry. J. Chromatogr. A 1347:63–71. https://doi.org/10.1016/j.chroma.2014.04.058.

Paltiel, O., Fedorova, G., Tadmor, G., Kleinstern, G., Maor, Y., Chefetz, B., 2016. Human exposure to wastewater-derived pharmaceuticals in fresh produce: a randomized controlled trial focusing on carbamazepine. Environ. Sci. Technol. 50:4476–4482. https://doi.org/10.1021/acs.est.5b06256.

Papa, E., Gramatica, P., 2010. QSPR as a support for the EU REACH regulation and rational design of environmentally safer chemicals: PBT identification from molecular structure. Green Chem. 12:836. https://doi.org/10.1039/b923843c.

Rastogi, T., Leder, C., Kümmerer, K., 2014. Designing green derivatives of β-blocker metoprolol: a tiered approach for green and sustainable pharmacy and chemistry. Chemosphere 111:493–499. https://doi.org/10.1016/j.chemosphere.2014.03.119.

Rastogi, T., Leder, C., Kümmerer, K., 2015. Re-designing of existing pharmaceuticals for environmental biodegradability: a tiered approach with β-blocker propranolol as an example. Environ. Sci. Technol. 11756–11763. https://doi.org/10.1021/acs.est.5b03051.

Ravyn, D., Ravyn, V., Lowney, R., Nasrallah, H.a., 2013. CYP450 pharmacogenetic treatment strategies for antipsychotics: a review of the evidence. Schizophr. Res. 149: 1–14. https://doi.org/10.1016/j.schres.2013.06.035.

Roberts, G., Myatt, G.J., Johnson, W.P., Cross, K.P., Blower, P.E., 2000. LeadScope: software for exploring large sets of screening data. J. Chem. Inf. Comput. Sci. 40:1302–1314. https://doi.org/10.1021/ci0000631.

Rodrigues, T., Dos Santos, C.G., Riposati, A., Barbosa, L.R.S., Di Mascio, P., Itri, R., Baptista, M.S., Nascimento, O.R., Nantes, I.I., 2006. Photochemically generated stable cation radical of phenothiazine aggregates in mildly acid buffered solutions. J. Phys. Chem. B 110:12257–12265. https://doi.org/10.1021/jp0605404.

Saiakhov, R., Chakravarti, S., Klopman, G., 2013. Effectiveness of CASE ultra expert system in evaluating adverse effects of drugs. Mol. Inf. 32:87–97. https://doi.org/10.1002/minf.201200081.

Saiakhov, R., Chakravarti, S., Sedykh, A., 2014. An improved workflow to perform in silico mutagenicity assessment of impurities as per ICH M7 guideline. Toxicol. Lett. 229: S164. https://doi.org/10.1016/j.toxlet.2014.06.563.

Salgado, R., Pereira, V.J., Carvalho, G., Soeiro, R., Gaffney, V., Almeida, C., Vale Cardoso, V., Ferreira, E., Benoliel, M.J., Ternes, T.A., Oehmen, A., Reis, M.A.M., Noronha, J.P., 2013. Photodegradation kinetics and transformation products of ketoprofen, diclofenac and atenolol in pure water and treated wastewater. J. Hazard. Mater. 244–245: 516–527. https://doi.org/10.1016/j.jhazmat.2012.10.039.

Sangion, A., Gramatica, P., 2016. PBT assessment and prioritization of contaminants of emerging concern: pharmaceuticals. Environ. Res. 147:297–306. https://doi.org/10.1016/j.envres.2016.02.021.

Santos, L.H.M.L.M., Araújo, A.N., Fachini, A., Pena, A., Delerue-matos, C., Montenegro, M.C.B.S.M., 2010. Ecotoxicological aspects related to the presence of pharmaceuticals in the aquatic environment. J. Hazard. Mater. 175:45–95. https://doi.org/10.1016/j.jhazmat.2009.10.100.

Sriram, D., Yogeeswari, P., 2010. Medicinal Chemistry. 2nd ed. Pearson, New Delhi, India.

Thanacoody, H.K.R., 2007. Thioridazine: resurrection as an antimicrobial agent? Br. J. Pharmacol. 64:566–574. https://doi.org/10.1111/j.1365-2125.2007.03021.x.

Thanacoody, R.B.H.K., 2011. Thioridazine: the good and the bad. Recent Pat. Antiinfect. Drug Discov. 6, 92–98.

Trautwein, C., Kümmerer, K., 2012a. Degradation of the tricyclic antipsychotic drug chlorpromazine under environmental conditions, identification of its main aquatic biotic and abiotic transformation products by LC-MSn and their effects on environmental bacteria. J. Chromatogr. B 889–890:24–38. https://doi.org/10.1016/j.jchromb.2012.01.022.

Trautwein, C., Kümmerer, K., 2012b. Ready biodegradability of trifluoromethylated phenothiazine drugs, structural elucidation of their aquatic transformation products, and identification of environmental risks studied by LC-MS^n and QSAR. Environ. Sci. Pollut. Res. 19:3162–3177. https://doi.org/10.1007/s11356-012-1002-1.

USEPA, 2012. U.S. EPA. Environmental protection agency EHAC. PBT profiler: a component of OPPT's P2 Frame work V 2.000; 2012. [WWW Document]. http://www.pbtprofiler.net/, Accessed date: 31 March 2015.

Vandermeersch, G., Lourenço, H.M., Alvarez-Muñoz, D., Cunha, S., Diogène, J., Cano-Sancho, G., Sloth, J.J., Kwadijk, C., Barcelo, D., Allegaert, W., Bekaert, K., Fernandes, J.O., Marques, A., Robbens, J., 2015. Environmental contaminants of emerging concern in seafood — European database on contaminant levels. Environ. Res. 1–17. https://doi.org/10.1016/j.envres.2015.06.011.

Please cite this article as: Wilde, M.L., et al., Combination of experimental and *in silico* methods for the assessment of the phototransformation products of the antipsychotic drug/metabolite Mesoridazine, Sci Total Environ (2017), https://doi.org/10.1016/j.scitotenv.2017.08.040

Wammer, K.H., Korte, A.R., Lundeen, R.A., Sundberg, J.E., McNeill, K., Arnold, W.A., 2013. Direct photochemistry of three fluoroquinolone antibacterials: norfloxacin, ofloxacin, and enrofloxacin. Water Res. 47:439–448. https://doi.org/10.1016/j.watres.2012.10.025.

Wang, X.H., Lin, A.Y.C., 2014. Is the phototransformation of pharmaceuticals a natural purification process that decreases ecological and human health risks? Environ. Pollut. 186:203–215. https://doi.org/10.1016/j.envpol.2013.12.007.

Werner, J.J., Arnold, W.A., Mcneill, K., 2006. Water hardness as a photochemical parameter: tetracycline photolysis as a function of calcium concentration, magnesium concentration, and pH. Environ. Sci. Technol. 40:7236–7241. https://doi.org/10.1021/es060337m.

Wilde, M.L., Menz, J., Trautwein, C., Leder, C., Kümmerer, K., 2016. Environmental fate and effect assessment of thioridazine and its transformation products formed by photodegradation. Environ. Pollut. 213:658–670. https://doi.org/10.1016/j.envpol.2016.03.018.

Wilde, M.L., Schneider, M., Kümmerer, K., 2017. Fenton process on single and mixture components of phenothiazine pharmaceuticals: assessment of intermediaries, fate, and preliminary ecotoxicity. Sci. Total Environ. 583:36–52. https://doi.org/10.1016/j.scitotenv.2016.12.184.

Wójcikowski, J., Maurel, P., Daniel, W.A., 2006. Characterization of human cytochrome p450 enzymes involved in the metabolism of the piperidine-type phenothiazine neuroleptic thioridazine. Drug Metab. Dispos. 34:471. https://doi.org/10.1124/dmd.105.006445.tion.

Wu, X., Conkle, J.L., Ernst, F., Gan, J., 2014. Treated wastewater irrigation: uptake of pharmaceutical and personal care products by common vegetables under field conditions. Environ. Sci. Technol. 48, 11286–11293.

Zepp, R.G., 1978. Quantum yields for reaction of pollutants in dilute aqueous solution. Environ. Sci. Technol. 12:1976–1978. https://doi.org/10.1021/es60139a010.

Zepp, R.G., Cline, D.M., 1977. Rates of direct photolysis in aquatic environment. Environ. Sci. Technol. 11:359–366. https://doi.org/10.1021/es60127a013.

Zhu, B., Zonja, B., Gonzalez, O., Sans, C., Pérez, S., Barceló, D., Esplugas, S., Xu, K., Qiang, Z., 2015. Degradation kinetics and pathways of three calcium channel blockers under UV irradiation. Water Res. 86:9–16. https://doi.org/10.1016/j.watres.2015.05.028.

Zonja, B., Pérez, S., Barceló, D., 2016. Human metabolite lamotrigine-N2-glucuronide is the principal source of lamotrigine-derived compounds in wastewater treatment plants and surface water. Environ. Sci. Technol. 50:154–164. https://doi.org/10.1021/acs.est.5b03691.

Please cite this article as: Wilde, M.L., et al., Combination of experimental and *in silico* methods for the assessment of the phototransformation products of the antipsychotic drug/metabolite Mesoridazine, Sci Total Environ (2017), https://doi.org/10.1016/j.scitotenv.2017.08.040